Hierarchical Coding for Cloud Storage: Topology-Adaptivity, Scalability, and Flexibility

Siyi Yang, *Student Member, IEEE*, Ahmed Hareedy, *Member, IEEE*, Robert Calderbank, *Fellow, IEEE*, and Lara Dolecek, *Senior Member, IEEE*

arXiv:2009.09146v1 [cs.IT] 19 Sep 2020

Abstract

In order to accommodate the ever-growing data from various, possibly independent, sources and the dynamic nature of data usage rates in practical applications, modern cloud data storage systems are required to be scalable, flexible, and heterogeneous. The recent rise of the blockchain technology is also moving various information systems towards decentralization to achieve high privacy at low costs. While codes with hierarchical locality have been intensively studied in the context of centralized cloud storage due to their effectiveness in reducing the average reading time, those for decentralized storage networks (DSNs) have not yet been discussed. In this paper, we propose a joint coding scheme where each node receives extra protection through the cooperation with nodes in its neighborhood in a heterogeneous DSN with any given topology. This work extends and subsumes our prior work on coding for centralized cloud storage. In particular, our proposed construction not only preserves desirable properties such as scalability and flexibility, which are critical in dynamic networks, but also adapts to arbitrary topologies, a property that is essential in DSNs but has been overlooked in existing works.

Index Terms

Joint hierarchical coding, cooperative data protection, decentralized storage networks, scalability, flexibility.

I. Introduction

In response to the rapidly growing demand of data management, cloud storage such as Microsoft Azure and Amazon Web Services have become among the most widely deployed public cloud services. In these centralized cloud services, a tech giant takes full custodianship over data of all its customers; this situation can result in expensive infrastructure maintenance and may lead to privacy violations. Decentralized storage networks (DSNs) such as Storj [3], in which no entity is solely responsible for all data, have emerged as a secure and economic alternative to centralized cloud services. DSNs are believed to be economically attractive since extra capacity can be afforded by utilizing idle storage space on devices at the edge of the network. Despite all advantages of decentralization, practical management of personal devices also faces challenges from component failures, high churn rates, heterogeneous bandwidths and link speeds, in addition to dynamic node balancing for content delivery of hot files [3]. While erasure correction (EC) codes are widely used to combat component failures, EC schemes that address the aforementioned issues are relatively overlooked. In this paper, we propose EC solutions that are tailored to tackle those challenges pertaining to DSNs.

Latency and reliability are among the most critical factors that customers care about in cloud storage. However, DSNs naturally impose numerous challenges on simultaneously maintaining low latency and high reliability. EC solutions with large block lengths are more resilient to large weight errors, but they simultaneously slow down the recovery for the more frequent cases where only few erasures occur. To reach a better trade-off between data reliability and latency, codes enabling multi-level access are desired. In these codes, any node is allowed to access different sets of helper nodes to retrieve the data, where the sizes of the sets get reduced if the number of erasures to be recovered is small enough. This architecture is referred to as codes with hierarchical localities. While hierarchical coding in the context of centralized storage [1], [4]–[11] has been intensively studied, codes for DSNs have been mostly discussed without considering localities [12]–[14].

More recently, codes with localities in multi-rack storage, a special case of DSNs, have also been investigated, where either the system is considered to be homogeneous [15]–[18], or the network topology has a simple structure [19], [20]. However, DSNs typically have more sophisticated topologies characterized by heterogeneity among bandwidths of communication links and erasure statistics of nodes due to the arbitrary and dynamic nature of practical networks [20]–[24]. Instead of solutions for simplified models, schemes that fit into any topology (a property referred to as **topology-adaptivity** later on) with customizable data lengths and redundancies are desired to exploit the existing resources.

Another major challenge for DSNs comes from the high churn rate, namely, participants join the network and leave without a predictable pattern. Therefore, it is essential for a DSN to enable its organic growth, i.e., enable expanding the backbone network to accommodate additional node operators, without rebuilding the entire infrastructure [25]; this property is referred to

Elements of this paper were presented in part at the IEEE Global Communications Conference, Waikoloa, Hawaii, USA, December 2019 [1], and at the IEEE International Symposium on Information Theory, Los Angeles, California, USA, June 2020 [2].

Siyi Yang and Lara Dolecek are with the Department of Electrical and Computer Engineering, University of California, Los Angeles, Los Angeles, CA 90095 USA (email: siyiyang@ucla.edu; dolecek@ee.ucla.edu).

Ahmed Hareedy and Robert Calderbank are with the Department of Electrical and Computer Engineering, Duke University, Durham, NC 27708 USA (email: ahmed.hareedy@duke.edu; robert.calderbank@duke.edu).

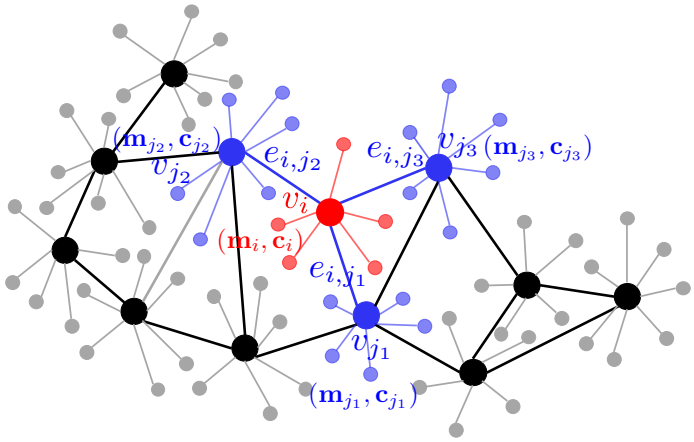


Fig. 1. Decentralized storage network (DSN). For the cluster with the master node v_i, message $\mathbf{m}_i$ is encoded to $\mathbf{c}_i$, and symbols of $\mathbf{c}_i$ are stored distributively among non-master nodes that are locally connected to v_i. In the figures after Fig. 1, we omit the local non-master nodes for clarity of figures.

as **scalability**. Moreover, data stored at certain nodes occasionally become hotter than anticipated, and the download rate can thus exceed the bandwidth limit. In such a scenario, dynamic node balancing is required for content delivery to reach a lower latency. In particular, the cloud (node) should be split into smaller clouds without worsening the global erasure correction capability or changing the remaining components. This property is referred to as **flexibility** and has been firstly investigated for dynamic data storage systems under the discussion of the so-called sum-rank codes [26]. However, sum-rank codes require a Galois field size that grows *exponentially* with the maximum local block length, which is a major obstacle to being implemented in real world applications [26].

In this paper, we strategically combine hierarchical locality and topological properties of a DSN. We develop a hierarchical coding scheme that is topologically-adaptive. The scheme is built upon our prior work on centralized cloud storage [1] and preserves desirable properties including scalability and flexibility. The Galois field size of this scheme grows *linearly* with the local block length. Our proposed coding scheme enables joint encoding and decoding of the data stored at all nodes such that nodes in a neighborhood cooperatively protect and validate their stored data collectively in the DSN. Cooperation in DSNs further improves the reliability since information propagates from more reliable nodes to less reliable nodes through paths connecting them.

The rest of the paper is organized as follows. In Section II, we introduce the DSN model and necessary preliminaries. In Section III, we define erasure correction (EC) hierarchies as well as their depth to systematically describe the maximal number of recoverable erasures corresponding to different access levels. We present a coding scheme with depth 1 that results in a better recovery speed compared with existing schemes that are not topologically-adaptive [19], [20]. We also discuss the recoverable erasure patterns of the proposed construction and show that our scheme enables correction of erasure patterns relevant to DSNs. In Section IV, we extend the single-level construction (depth 1) to have higher-level cooperation. In the hierarchical scheme, the cooperation between nodes in the DSN is described by the so-called **cooperation graphs**. We also present sufficient conditions on any graph to be a cooperation graph, and refer to graphs satisfying these conditions as **compatible graphs**. In Section V, we first present an algorithm that searches for a cooperation graph on any DSN with a given topology. Next, we show that our coding scheme supports scalability and flexibility. Finally, we summarize our results in Section VI.

II. Notation and Preliminaries

In this section, we discuss the model and mathematical representation of a DSN, as well as necessary preliminaries. Throughout the remainder of this paper, $[N]$ refers to $\{1, 2, \ldots, N\}$. For a vector $\mathbf{v}$ of length n, v_i, $1 \leq i \leq n$, represents the i-th component of $\mathbf{v}$, and $\mathbf{v}[a:b] = (v_a, \ldots, v_b)$. For a matrix $\mathbf{M}$ of size $a \times b$, $\mathbf{M}[i_1 : i_2, j_1 : j_2]$ represents the sub-matrix $\mathbf{M}'$ of $\mathbf{M}$ such that $(\mathbf{M}')_{i-i_1+1, j-j_1+1} = (\mathbf{M})_{i,j}$, $i \in [i_1 : i_2]$, $j \in [j_1 : j_2]$. For vectors $\mathbf{u}$ and $\mathbf{v}$ of the same length p, $\mathbf{u} \succ \mathbf{v}$ and $\mathbf{u} \prec \mathbf{v}$ means $u_i > v_i$ and $u_i < v_i$, for all $i \in [p]$, respectively; $\mathbf{u} \succeq \mathbf{v}$ and $\mathbf{u} \preceq \mathbf{v}$ means $u_i \geq v_i$ and $u_i \leq v_i$, for all $i \in [p]$, respectively. For any $m, n \in \mathbb{N}$, an identity matrix of size $n \times n$ is denoted by $\mathbf{I}_n$, and a zero matrix of size $m \times n$ is denoted by $\mathbf{0}_{m \times n}$. For any $q \in \mathbb{N}$, GF(q) refers to a Galois field with size q. In this paper, we constrain q to be a power of 2.

A. Decentralized Storage Network

In a DSN, nodes are typically partitioned into distributed clusters of nodes, where each cluster has a "master node" that functions in this cluster similar to that of a central node in a centralized network, which is what the "decentralization" refers to. As shown in Fig. 1, each master node, represented by big bold-colored nodes, communicates with both its neighboring master nodes and other nodes in the cluster it belongs to, whereas each non-master node, represented by small light-colored nodes, only communicates with the master node of the cluster it belongs to. For the cluster with the master node v_i, message

$\mathbf{m}_i$ is encoded to $\mathbf{c}_i$, and symbols of $\mathbf{c}_i$ are stored distributively among non-master nodes that are locally connected to v_i. For clarity and simplicity of figures and notation, we omit the non-master nodes in figures after Fig. 1. We then refer to master nodes and the communication links among them by "nodes" and "edges", respectively, in the remainder of this paper.

As shown in Fig. 1, a DSN is modeled as a graph $G(V, E)$, where V and E denote the set of nodes (master only) and edges, respectively. Codewords are stored among the nodes in a cluster. A failed node in a cluster is regarded as an erased symbol in the codeword stored at this cluster. A cluster is represented in G by its master node $v_i \in V$ solely. Each edge $e_{i,j} \in E$ represents a communication link connecting node v_i and node v_j, through which v_i and v_j are allowed to exchange information. Denote the set of all neighbors of node v_i by $\mathcal{N}_i$, e.g., $\mathcal{N}_i = \{v_{j_1}, v_{j_2}, v_{j_3}\}$ in Fig. 1, and refer to it as the **neighborhood** of node v_i. Messages $\{\mathbf{m}_i\}_{v_i \in V}$ are jointly encoded as $\{\mathbf{c}_i\}_{v_i \in V}$, and $\mathbf{c}_i$ is stored at the cluster of nodes containing v_i. For simplicity, we instead say "$\mathbf{c}_i$ is stored at node v_i" in the rest of the paper.

For a DSN denoted by $G(V, E)$, let $p = |V|$. Suppose G is associated with a tuple $(\mathbf{n}, \mathbf{k}, \mathbf{r}) \in (\mathbb{N}^p)^3$, where $\mathbf{k}, \mathbf{r} \succ \mathbf{0}$ and $\mathbf{n} = \mathbf{k} + \mathbf{r}$. Note that k_i represents the length of the message $\mathbf{m}_i$ associated with $v_i \in V$; n_i and r_i denote the length of $\mathbf{c}_i$ stored at v_i and its syndrome, respectively. Let $\mathbf{m} = (\mathbf{m}_1, \mathbf{m}_2, \ldots, \mathbf{m}_p)$, and $\mathbf{c} = (\mathbf{c}_1, \mathbf{c}_2, \ldots, \mathbf{c}_p)$. A set $\mathcal{C}$ is called an $(n, k, d)_q$-code if $\mathcal{C} \subset \mathrm{GF}(q)^n$, $\dim(\mathcal{C}) = k$, and $\min_{\mathbf{c}, \mathbf{c}' \in \mathcal{C}, \mathbf{c} \neq \mathbf{c}'} d_{\mathrm{H}}(\mathbf{c}, \mathbf{c}') - 1 = d$, where d_{H} refers to the Hamming distance. We next define a family of codes with double-level access. Note that our discussion is restricted to linear block codes.

B. Cauchy Matrices

Before we describe the constructions in detail, we first introduce the so-called **Cauchy matrices** that are used as major components in the generator matrices of our codes. Codes based on Cauchy matrices, the so-called Cauchy Reed-Solomon (CRS) codes, have been studied in [27], [28]. CRS codes present desirable properties, as discussed later, and have been proposed to be applied to distributed storage systems in [29], [30]. In our work, we further exploit the scaling property of CRS codes, which makes them an ideal choice to accommodate hierarchical access on arbitrarily deployed nodes in DSNs.

Definition 1. (Cauchy matrix) *Let $s, t \in \mathbb{N}$ and $\mathrm{GF}(q)$ be a Galois field of size q. Suppose $a_1, \ldots, a_s, b_1, \ldots, b_t$ are $s + t$ distinct elements in $\mathrm{GF}(q)$. The following matrix is known as a **Cauchy matrix**,*

$$\begin{bmatrix} \frac{1}{a_1 - b_1} & \frac{1}{a_1 - b_2} & \cdots & \frac{1}{a_1 - b_t} \\ \frac{1}{a_2 - b_1} & \frac{1}{a_2 - b_2} & \cdots & \frac{1}{a_2 - b_t} \\ \vdots & \vdots & \ddots & \vdots \\ \frac{1}{a_s - b_1} & \frac{1}{a_s - b_2} & \cdots & \frac{1}{a_s - b_t} \end{bmatrix}.$$

*We denote this matrix by $\mathbf{Y}(a_1, \ldots, a_s; b_1, \ldots, b_t)$, and refer to sequences $(a_1, a_2, \ldots, a_s)$, $(b_1, b_2, \ldots, b_t)$ as the **row indicator** and the **column indicator** of the specified Cauchy matrix, respectively.*

Cauchy matrices possess desirable properties that make them an ideal alternative to Vandermonde matrices, the major components of the parity-check matrices of Reed-Solomon (RS) codes, as the parity-computing (non-systematic) components in systematic generator matrices of some maximum distance separable (MDS) codes with low encoding and decoding complexities [29]. Cauchy matrices are **totally invertible**, i.e., every square sub-matrix of a Cauchy matrix is invertible. Therefore, horizontally concatenating a Cauchy matrix with another Cauchy matrix having an identical row indicator but a non-overlapping column indicator results in a third Cauchy matrix. Similarly, vertically concatenating a Cauchy matrix with another Cauchy matrix having an identical column indicator but a non-overlapping row indicator also results in a third Cauchy matrix. This property, referred to as the scaling property previously, is desirable for hierarchical access in topology-adaptive DSNs. Moreover, Lemma 1 presents another useful property about Cauchy matrices, which will be used repeatedly in this paper.

Lemma 1. *Let $s, t, r \in \mathbb{N}$ such that $t - s < r \leq t$, and $\mathbf{A} \in \mathrm{GF}(q)^{s \times t}$. If $\mathbf{A}$ is a Cauchy matrix, then the following matrix $\mathbf{M}$ is a parity-check matrix of an $(s + r, s + r - t, t + 1)_q$-code*[1]*,*

$$\mathbf{M} = \begin{bmatrix} \mathbf{A} \\ -\mathbf{I}_r \ \mathbf{0}_{r \times (t-r)} \end{bmatrix}^{\mathrm{T}}.$$

Proof. The parity-check matrix of an $(s+r, s+r-t, t+1)_q$-code satisfies the property that every t columns of this matrix are linearly independent. Therefore, we only need to prove that every t rows of $\mathbf{M}^{\mathrm{T}}$ are linearly independent. We prove Lemma 1 by contradiction. Suppose there exist t rows from $\mathbf{M}^{\mathrm{T}}$ that are linearly dependent. Suppose a of these linearly dependent rows $\mathbf{r}_1, \mathbf{r}_2, \ldots, \mathbf{r}_a$ are from $\mathbf{A}$, and the other $t - a$ rows $\mathbf{r}_{a+1}, \mathbf{r}_{a+2}, \ldots, \mathbf{r}_t$ are from $\left[-\mathbf{I}_r \ \mathbf{0}_{r \times (t-r)}\right]$, where $0 \leq t - a \leq r$. Suppose the entries with -1 in $\mathbf{r}_{a+1}, \mathbf{r}_{a+2}, \ldots, \mathbf{r}_t$ are located in the $i_1, i_2 \ldots, i_{t-a}$-th columns of $\mathbf{M}^{\mathrm{T}}$, then $i_p \leq r$ for all $1 \leq p \leq t - a$. Observe that $[t]$ is the set of indices of all columns in $\mathbf{M}^{\mathrm{T}}$. Suppose $[t] \setminus \{i_1, i_2, \ldots, i_{t-a}\} = \{j_1, j_2, \ldots, j_a\}$. Then, the $a \times a$ sub-matrix of the intersection of the rows $\mathbf{r}_1, \mathbf{r}_2, \ldots, \mathbf{r}_a$ and the $j_1, j_2, \ldots, j_a$-th columns of $\mathbf{A}$ is singular. A contradiction. ∎

[1]Note that when q is a power of 2, the minus operand can be removed, as shown in Example 1, since subtraction and addition are equivalent on the Galois field $\mathrm{GF}(q)$ in this case.

C. Locality of Interleaved Cauchy Reed Solomon Codes

A code is **systematic** if the codeword contains a segment that is identical to the message being encoded. For a linear block code, systematic encoding of messages with length k is performed via a generator matrix containing a $k \times k$ submatrix being the identity matrix $\mathbf{I}_k$. Systematic codes are of interest because of their low complexity mapping from any valid codeword to the message it represents, as well as their low encoding complexity due to the fact that only parities need extra calculation steps. Based on the aforementioned notation, a systematic generator matrix of a code on $G(V, E)$ has the following structure:

$$\mathbf{G} = \left[\begin{array}{c|c|c|c|c|c|c} \mathbf{I}_{k_1} & \mathbf{A}_{1,1} & \mathbf{0} & \mathbf{A}_{1,2} & \dots & \mathbf{0} & \mathbf{A}_{1,p} \\ \hline \mathbf{0} & \mathbf{A}_{2,1} & \mathbf{I}_{k_2} & \mathbf{A}_{2,2} & \dots & \mathbf{0} & \mathbf{A}_{2,p} \\ \hline \vdots & \vdots & \vdots & \vdots & \ddots & \vdots & \vdots \\ \hline \mathbf{0} & \mathbf{A}_{p,1} & \mathbf{0} & \mathbf{A}_{p,2} & \dots & \mathbf{I}_{k_p} & \mathbf{A}_{p,p} \end{array}\right], \tag{1}$$

where all elements are from a Galois field GF(q), $q = 2^\theta$ and $\theta \geq 2$.

Following the notation in the previous subsections, the codeword at node v_i is $\mathbf{c}_i = (\mathbf{m}_i, \sum_{j\in[p]} \mathbf{m}_j\mathbf{A}_{j,i})$, and it has two parts. We call $\mathbf{m}_i$ the systematic part, and $\sum_{j\in[p]} \mathbf{m}_j\mathbf{A}_{j,i}$ the **local parities** of $\mathbf{c}_i$. More specifically, we refer to $\sum_{j\in[p],j\neq i} \mathbf{m}_j\mathbf{A}_{j,i}$, $\mathbf{m}_i\mathbf{A}_{i,i}$ as the **additional local parities** and the **original local parities** at v_i, respectively. For any $j \in [p]$, $j \neq i$, symbols in $\mathbf{m}_i\mathbf{A}_{i,j}$ are referred to as the **cross parities** of v_i from node v_j. Note that by saying "parities" we actually mean "parity symbols". We use these two terms interchangeably in the remaining text.

The submatrices $\{\mathbf{A}_{i,j}\}_{i,j\in[p]}$ in our construction are either zero matrices, Cauchy matrices, or products of Cauchy matrices. For this reason, we call codes represented by a generator matrix in (1) as **interleaved Cauchy Reed Solomon (CRS) codes**. The primary property of interleaved CRS codes is that each local message $\mathbf{m}_i$ is to be obtained locally by only accessing the codeword $\mathbf{c}_i$ stored at v_i if the number of erasures in $\mathbf{c}_i$ does not exceed an upper bound that is determined by some local parameters. We next provide an exemplary construction, Construction 1, to illustrate the locality of interleaved CRS codes.

Construction 1. *(Interleaved CRS codes) Let $p \in \mathbb{N}$, $k_1, k_2, \dots, k_p \in \mathbb{N}$, $n_1, n_2, \dots, n_p \in \mathbb{N}$, $\delta_1, \delta_2, \dots, \delta_p \in \mathbb{N}$, with $r_x = n_x - k_x > 0$ for all $x \in [p]$. Let $P = ([p] \times [p]) \setminus \{(i, i)\}_{i\in[p]}$, and $I \subseteq P$ is such that for all $(x, y) \in I$, $\mathbf{A}_{x,y}$ is non-zero. Let $I_x = \{i : (x, i) \in I\}$, for each $x \in [p]$, and suppose $I_x = \{i_1, i_2, \cdots, i_{|I_x|}\}$. Let $\delta'_x = \sum_{y\in I_x} \delta_y$, for all $x \in [p]$. Let* GF(q) *be a Galois field such that $q \geq \max_{x\in[p]}\{n_x + \delta'_x\}$.*

For each $x \in [p]$, let $a_{x,i}$, $i \in [k_x + \delta_x]$, and $b_{x,j}$, $j \in [r_x - \delta_x + \delta'_x]$, be distinct elements of GF(q). *Consider the Cauchy matrix $\mathbf{T}_x \in$ GF$(q)^{(k_x+\delta_x)\times(r_x-\delta_x+\delta'_x)}$ such that $\mathbf{T}_x = \mathbf{Y}(a_{x,1}, \dots, a_{x,k_x+\delta_x}; b_{x,1}, \dots, b_{x,r_x-\delta_x+\delta'_x})$. For each $x \in [p]$, we obtain $\{\mathbf{B}_{x,i}\}_{i\in I_x}$, $\mathbf{U}_x$, $\mathbf{A}_{x,x}$, according to the following partition of $\mathbf{T}_x$:*

$$\mathbf{T}_x = \left[\begin{array}{c|c|c|c} \mathbf{A}_{x,x} & \mathbf{B}_{x,i_1} & \dots & \mathbf{B}_{x,i_{|I_x|}} \\ \hline \mathbf{U}_x & \multicolumn{3}{c}{\mathbf{Z}_x} \end{array}\right], \tag{2}$$

where $\mathbf{A}_{x,x} \in$ GF$(q)^{k_x\times r_x}$, $\mathbf{B}_{x,i} \in$ GF$(q)^{k_x\times\delta_i}$, $\mathbf{U}_x \in$ GF$(q)^{\delta_x\times r_x}$. Moreover, let $\mathbf{A}_{x,y} = \mathbf{B}_{x,y}\mathbf{U}_y$, for $(x, y) \in I$; let $\mathbf{A}_{x,y} = \mathbf{0}_{k_x\times r_y}$, for $(x, y) \in P \setminus I$.

Matrices $\mathbf{A}_{x,x}$ and $\mathbf{A}_{x,y}$ are substituted in $\mathbf{G}$ specified in (1), for all $x, y \in [p]$. Let $\mathcal{C}_1$ represent the code with the generator matrix $\mathbf{G}$.

Following the notation in Subsection II-A, suppose in a DSN that is implemented with a code specified in Construction 1, all nodes are able to communicate with each other. For all $x \in [p]$, let $d_{x,1}$, $d_{x,2}$ represent the maximum number of erasures that node v_x can tolerate with local access to the codeword $\mathbf{c}_x$, and global access to all the codewords $\{\mathbf{c}_x\}_{x\in[p]}$, respectively. Lemma 2 presents the value of the local and the global correction capabilities of codes proposed in Construction 1. Note that even though $\mathbf{m}_j\mathbf{A}_{j,i} = \mathbf{m}_j\mathbf{B}_{j,i}\mathbf{U}_i$ gives the explicit cross parities, symbols resulting from $\mathbf{m}_j\mathbf{B}_{j,i}$ can accurately be seen as the cross parities too since they constitute a set of independent linear combinations of message symbols, and they contain all the information node v_j provides to node v_i, for all $v_i, v_j \in V, i \neq j$. Therefore, in the remainder of this paper, we also refer to $\mathbf{m}_j\mathbf{B}_{j,i}$ as the cross parities or the cross parity symbols for simplicity.

Lemma 2. *In code $\mathcal{C}_1$ specified in Construction 1, $d_{x,1} = r_x - \delta_x$, $d_{x,2} = r_x + \delta'_x$, for $x \in [p]$.*

Proof. For each $x \in [p]$, define $\mathbf{y}_x = \sum_{y\in I_x} \mathbf{m}_y\mathbf{B}_{y,x}$. It follows from $\mathbf{mG} = \mathbf{c}$ and (1) that for $x \in [p]$, $\mathbf{c}_x = [\mathbf{m}_x, \mathbf{m}_x\mathbf{A}_{x,x} + \mathbf{y}_x\mathbf{U}_x]$. Define the local parity-check matrix $\mathbf{H}^{\mathrm{L}}_x$ and the global parity-check matrix $\mathbf{H}^{\mathrm{G}}_x$, for each $x \in [p]$, as follows:

$$\mathbf{H}^{\mathrm{G}}_x = \left[\begin{array}{c|c|c|c} \mathbf{A}_{x,x} & \mathbf{B}_{x,i_1} & \dots & \mathbf{B}_{x,i_{|I_x|}} \\ \hline -\mathbf{I}_{r_x} & \multicolumn{3}{c}{\mathbf{0}_{r_x\times\delta'_x}} \end{array}\right]^{\mathrm{T}}, \ \mathbf{H}^{\mathrm{L}}_x = \left[\begin{array}{c} \mathbf{A}_{x,x} \\ -\mathbf{I}_{r_x} \\ \mathbf{U}_x \end{array}\right]^{\mathrm{T}}.$$

We next prove the equations of the local correction capability $d_{x,1} = r_x - \delta_x$ and the global correction capability $d_{x,2} = r_x + \delta'_x$ using $\mathbf{H}^{\mathrm{L}}_x$ and $\mathbf{H}^{\mathrm{G}}_x$, $x \in [p]$.

To prove the equation of the local correction capability, let $\tilde{\mathbf{c}}_x = [\mathbf{c}_x, \mathbf{y}_x]$. Then, one can show that $\tilde{\mathbf{c}}_x$ belongs to a code $\mathcal{C}^{\mathrm{L}}_x$ with the local parity-check matrix $\mathbf{H}^{\mathrm{L}}_x$. From Lemma 1, $\mathcal{C}^{\mathrm{L}}_x$ is an $(n_x + \delta_x, k_x, r_x + 1)_q$-code. Therefore, any r_x erasures

TABLE I
POLYNOMIAL AND BINARY REPRESENTATION OF GF(2^4)

0	0000	β^4	1100	β^8	1010	β^{12}	1111
β	0100	β^5	0110	β^9	0101	β^{13}	1011
β^2	0010	β^6	0011	β^{10}	1110	β^{14}	1001
β^3	0001	β^7	1101	β^{11}	0111	$\beta^{15}=1$	1000

$$\mathbf{T}_1=\mathbf{T}_2=\left[\begin{array}{c|c}\mathbf{A}_{1,1} & \mathbf{B}_{1,2}\\ \hline \mathbf{U}_1 & \mathbf{Z}_1\end{array}\right]=\left[\begin{array}{c|c}\mathbf{A}_{2,2} & \mathbf{B}_{2,1}\\ \hline \mathbf{U}_2 & \mathbf{Z}_2\end{array}\right]=\left[\begin{array}{cccc|c}\frac{1}{\beta-\beta^8} & \frac{1}{\beta-\beta^9} & \frac{1}{\beta-\beta^{10}} & \frac{1}{\beta-\beta^{11}} & \\ \frac{1}{\beta^2-\beta^8} & \frac{1}{\beta^2-\beta^9} & \frac{1}{\beta^2-\beta^{10}} & \frac{1}{\beta^2-\beta^{11}} & \\ \frac{1}{\beta^3-\beta^8} & \frac{1}{\beta^3-\beta^9} & \frac{1}{\beta^3-\beta^{10}} & \frac{1}{\beta^3-\beta^{11}} & \\ \hline \frac{1}{\beta^7-\beta^8} & \frac{1}{\beta^7-\beta^9} & \frac{1}{\beta^7-\beta^{10}} & \frac{1}{\beta^7-\beta^{11}} & \end{array}\right]=\left[\begin{array}{cccc|c}\beta^5 & \beta^{12} & \beta^7 & \beta^9 & \\ 1 & \beta^4 & \beta^{11} & \beta^6 & \\ \beta^2 & \beta^{14} & \beta^3 & \beta^{10} & \\ \hline \beta^4 & 1 & \beta^9 & \beta^7 & \end{array}\right]. \quad (3)$$

in $\tilde{\mathbf{c}}_x$ are correctable. Provided that $\mathbf{y}_x$ has length δ_x, we can consider the entries of $\mathbf{y}_x$ as erasures, and thus any $(r_x-\delta_x)$ erasures in the remaining part of $\tilde{\mathbf{c}}_x$, i.e., $\mathbf{c}_x$, can be corrected. Therefore, $d_{x,1}=r_x-\delta_x$.

To prove the equation of the global correction capability, assume all the local codewords except for $\mathbf{c}_x$ are successfully decodable locally. For each $x\in[p]$, let $\mathbf{s}_x=\left[\mathbf{m}_x\mathbf{B}_{x,i_1},\ldots,\mathbf{m}_x\mathbf{B}_{x,i_{|I_x|}}\right]$ and $\bar{\mathbf{c}}_x=\mathbf{c}_x-[\mathbf{0}_{k_x},\mathbf{y}_x\mathbf{U}_x]$. Then, one can show that $\mathbf{H}_x^{\mathrm{G}}\bar{\mathbf{c}}_x^{\mathrm{T}}=[\mathbf{0}_{r_x},\mathbf{s}_x]^{\mathrm{T}}$. From Lemma 1 and from the construction of $\mathbf{H}_x^{\mathrm{G}}$, any $(r_x+\delta'_x)$ erasures in $\bar{\mathbf{c}}_x$ are correctable, and thus $(r_x+\delta'_x)$ erasures in $\mathbf{c}_x$ are also correctable. Therefore, $d_{x,2}=r_x+\delta'_x$. ■

Next, we give an example of Construction 1 where $I=P$. Namely, all the $\mathbf{A}_{x,y}$, $(x,y)\in P$, are non-zero matrices. Example 1 also demonstrates how erasures are corrected.

Example 1. *Let $q=2^4$, $p=2$, $r=r_1=r_2=3$, $\delta=\delta_1=\delta_2=1$, $k=k_1=k_2=3$, $n=n_1=n_2=k+r=6$, $\delta'=\delta'_1=\delta'_2=\delta_1+\delta_2-\delta=1$. Then, $d_1=r-\delta'=3-1=2$, $d_2=r+\delta'=3+1=4$. Choose a primitive polynomial of degree 4 over* GF(2)*: $g(X)=X^4+X+1$. Let β be a root of $g(X)$. Then, β is a primitive element of* GF(2^4). *The binary representation of all the symbols in* GF(2^4) *is provided in Table I.*

Let $\mathbf{A}_{1,1}=\mathbf{A}_{2,2}$, $\mathbf{B}_{1,2}=\mathbf{B}_{2,1}$, $\mathbf{U}_1=\mathbf{U}_2$, and $\mathbf{T}_1=\mathbf{T}_2$ as specified in (3). Therefore,

$$\mathbf{A}_{1,2}=\mathbf{A}_{2,1}=\mathbf{B}_{2,1}\mathbf{U}_1=\begin{bmatrix}\beta^{13} & \beta^9 & \beta^3\\ \beta^{10} & \beta^6 & 1\\ \beta^{14} & \beta^{10} & \beta^4\end{bmatrix}.$$

Then, the generator matrix $\mathbf{G}$ is specified as follows,

$$\left[\begin{array}{ccc|ccc|ccc|ccc}1&0&0&\beta^5&\beta^{12}&\beta^7&0&0&0&\beta^{13}&\beta^9&\beta^3\\ 0&1&0&1&\beta^4&\beta^{11}&0&0&0&\beta^{10}&\beta^6&1\\ 0&0&1&\beta^2&\beta^{14}&\beta^3&0&0&0&\beta^{14}&\beta^{10}&\beta^4\\ \hline 0&0&0&\beta^{13}&\beta^9&\beta^3&1&0&0&\beta^5&\beta^{12}&\beta^7\\ 0&0&0&\beta^{10}&\beta^6&1&0&1&0&1&\beta^4&\beta^{11}\\ 0&0&0&\beta^{14}&\beta^{10}&\beta^4&0&0&1&\beta^2&\beta^{14}&\beta^3\end{array}\right]=\left[\begin{array}{cccc}\mathbf{I}_{k_1}&\mathbf{A}_{1,1}&\mathbf{0}_{k_1\times k_2}&\mathbf{A}_{1,2}\\ \mathbf{0}_{k_2\times k_1}&\mathbf{A}_{2,1}&\mathbf{I}_{k_2}&\mathbf{A}_{2,2}\end{array}\right].$$

Suppose $\mathbf{m}_1=(1,\beta,\beta^2)$ and $\mathbf{m}_2=(\beta,1,0)$. Thus, $\mathbf{c}_1=(1,\beta,\beta^2,\beta^{14},0,0)$ and $\mathbf{c}_2=(\beta,1,0,\beta^6,0,\beta^{13})$. Moreover, $\mathbf{H}_1^{\mathrm{L}}$ and $\mathbf{H}_1^{\mathrm{G}}$ are specified as follows,

$$\mathbf{H}_1^{\mathrm{G}}=\begin{bmatrix}\beta^5&\beta^{12}&\beta^7&\beta^9\\ 1&\beta^4&\beta^{11}&\beta^6\\ \beta^2&\beta^{14}&\beta^3&\beta^{10}\\ 1&0&0&0\\ 0&1&0&0\\ 0&0&1&0\end{bmatrix}^{\mathrm{T}},\ \mathbf{H}_1^{\mathrm{L}}=\begin{bmatrix}\beta^5&\beta^{12}&\beta^7\\ 1&\beta^4&\beta^{11}\\ \beta^2&\beta^{14}&\beta^3\\ 1&0&0\\ 0&1&0\\ 0&0&1\\ \beta^4&1&\beta^9\end{bmatrix}^{\mathrm{T}}.$$

According to Construction 1, $\mathbf{G}$ is the generator matrix of a double-level accessible code that corrects 2 local erasures by local access, and corrects 2 extra erasures within a single cloud by global access. In the following, we denote the version of $\mathbf{c}_1$ having erasures by $\mathbf{c}'_1$, and erased symbols by e_i, $i\in\mathbb{N}$.

As an example of decoding by local access, suppose $\mathbf{c}'_1=(1,e_1,\beta^2,e_2,0,0)$. Then, the erased elements of $\tilde{\mathbf{c}}_1=(1,e_1,\beta^2,e_2,0,0,e_3)$ can be retrieved using $\mathbf{H}_1^{\mathrm{L}}$ as its parity-check matrix. In particular, we solve $\mathbf{H}_1^{\mathrm{L}}\tilde{\mathbf{c}}_1^{\mathrm{T}}=(0,0,0)^{\mathrm{T}}$ for e_1,e_2,e_3 and obtain $(e_1,e_2,e_3)=(\beta,\beta^{14},\beta^7)$. Therefore, we have decoded $\mathbf{c}_1$ successfully.

As an example of decoding by global access, suppose $\mathbf{c}'_1=(e_1,e_2,\beta^2,e_3,e_4,0)$, and suppose $\mathbf{c}_2$ has been decoded successfully as $\mathbf{c}_2=(\beta,1,0,\beta^6,0,\beta^{13})$, which implies that $\mathbf{m}_1\mathbf{B}_{1,2}\mathbf{U}_2=(\beta^6,0,\beta^{13})-\beta\cdot(\beta^5,\beta^{12},\beta^7)-1\cdot(1,\beta^4,\beta^{11})=(1,\beta^{11},\beta^5)$. Since $\mathbf{U}_2=(\beta^4,1,\beta^9)$, we obtain $\mathbf{m}_1\mathbf{B}_{1,2}=\beta^{11}$. Moreover, we compute $\mathbf{m}_2\mathbf{B}_{2,1}\mathbf{U}_1=(\beta^{11},\beta^7,\beta)$. Let

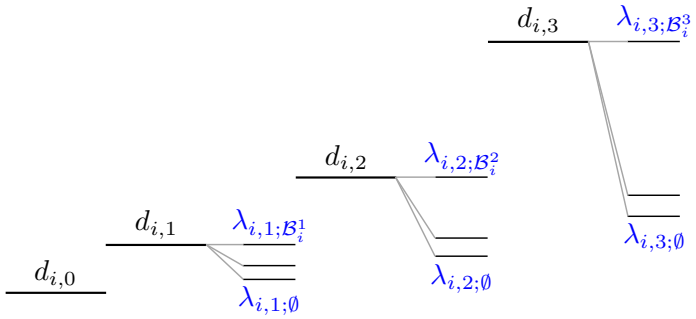


Fig. 2. EC hierarchy of node $v_i \in V$. The values $d_{i,0}$ and $d_{i,\ell}$, $1 \leq \ell \leq 3$, represent the maximum number of erasures v_i can tolerate in the local decoding, and decoding with the assistance of the 1-st to the ℓ-th level cooperations of the codeword $\mathbf{c}_i$, i.e., cooperating with nodes in $\mathcal{A}_i^\ell$, respectively. However, even for a fixed $\mathcal{A}_i^\ell$, different sets $\mathcal{W}$ of nodes that are recovered in $\mathcal{B}_i^\ell$ may also result in different EC capabilities; we refer to them as $(\lambda_{i,\ell;\mathcal{W}})$, $\varnothing \subseteq \mathcal{W} \subseteq \mathcal{B}_i^\ell$.

1	2	3	4	5	6	7	8	9	10	11	12
$\mathbf{A}_{1,1}$	$\mathbf{B}_{1,2}\mathbf{U}_2$	$\mathbf{0}$	$\mathbf{0}$	$\mathbf{0}$	$\mathbf{0}$	$\mathbf{0}$	$\mathbf{0}$	$\mathbf{0}$	$\mathbf{0}$	$\mathbf{0}$	$\mathbf{0}$
$\mathbf{B}_{2,1}\mathbf{U}_1$	$\mathbf{A}_{2,2}$	$\mathbf{B}_{2,3}\mathbf{U}_3$	$\mathbf{0}$	$\mathbf{B}_{2,5}\mathbf{U}_5$	$\mathbf{0}$	$\mathbf{0}$	$\mathbf{0}$	$\mathbf{0}$	$\mathbf{0}$	$\mathbf{0}$	$\mathbf{0}$
$\mathbf{0}$	$\mathbf{B}_{3,2}\mathbf{U}_2$	$\mathbf{A}_{3,3}$	$\mathbf{B}_{3,4}\mathbf{U}_4$	$\mathbf{0}$	$\mathbf{0}$	$\mathbf{0}$	$\mathbf{0}$	$\mathbf{0}$	$\mathbf{0}$	$\mathbf{0}$	$\mathbf{0}$
$\mathbf{0}$	$\mathbf{0}$	$\mathbf{B}_{4,3}\mathbf{U}_3$	$\mathbf{A}_{4,4}$	$\mathbf{B}_{4,5}\mathbf{U}_5$	$\mathbf{B}_{4,6}\mathbf{U}_6$	$\mathbf{0}$	$\mathbf{0}$	$\mathbf{0}$	$\mathbf{0}$	$\mathbf{0}$	$\mathbf{0}$
$\mathbf{0}$	$\mathbf{B}_{5,2}\mathbf{U}_2$	$\mathbf{0}$	$\mathbf{B}_{5,4}\mathbf{U}_4$	$\mathbf{A}_{5,5}$	$\mathbf{B}_{5,6}\mathbf{U}_6$	$\mathbf{0}$	$\mathbf{B}_{5,8}\mathbf{U}_8$	$\mathbf{0}$	$\mathbf{0}$	$\mathbf{0}$	$\mathbf{0}$
$\mathbf{0}$	$\mathbf{0}$	$\mathbf{0}$	$\mathbf{B}_{6,4}\mathbf{U}_4$	$\mathbf{B}_{6,5}\mathbf{U}_5$	$\mathbf{A}_{6,6}$	$\mathbf{B}_{6,7}\mathbf{U}_7$	$\mathbf{0}$	$\mathbf{0}$	$\mathbf{0}$	$\mathbf{0}$	$\mathbf{0}$
$\mathbf{0}$	$\mathbf{0}$	$\mathbf{0}$	$\mathbf{0}$	$\mathbf{0}$	$\mathbf{B}_{7,6}\mathbf{U}_6$	$\mathbf{A}_{7,7}$	$\mathbf{B}_{7,8}\mathbf{U}_8$	$\mathbf{B}_{7,9}\mathbf{U}_9$	$\mathbf{0}$	$\mathbf{B}_{7,11}\mathbf{U}_{11}$	$\mathbf{0}$
$\mathbf{0}$	$\mathbf{0}$	$\mathbf{0}$	$\mathbf{0}$	$\mathbf{B}_{8,5}\mathbf{U}_5$	$\mathbf{0}$	$\mathbf{B}_{8,7}\mathbf{U}_7$	$\mathbf{A}_{8,8}$	$\mathbf{B}_{8,9}\mathbf{U}_9$	$\mathbf{0}$	$\mathbf{0}$	$\mathbf{0}$
$\mathbf{0}$	$\mathbf{0}$	$\mathbf{0}$	$\mathbf{0}$	$\mathbf{0}$	$\mathbf{0}$	$\mathbf{B}_{9,7}\mathbf{U}_7$	$\mathbf{B}_{9,8}\mathbf{U}_8$	$\mathbf{A}_{9,9}$	$\mathbf{B}_{9,10}\mathbf{U}_{10}$	$\mathbf{0}$	$\mathbf{0}$
$\mathbf{0}$	$\mathbf{0}$	$\mathbf{0}$	$\mathbf{0}$	$\mathbf{0}$	$\mathbf{0}$	$\mathbf{0}$	$\mathbf{0}$	$\mathbf{B}_{10,9}\mathbf{U}_9$	$\mathbf{A}_{10,10}$	$\mathbf{B}_{10,11}\mathbf{U}_{11}$	$\mathbf{B}_{10,12}\mathbf{U}_{12}$
$\mathbf{0}$	$\mathbf{0}$	$\mathbf{0}$	$\mathbf{0}$	$\mathbf{0}$	$\mathbf{0}$	$\mathbf{B}_{11,7}\mathbf{U}_7$	$\mathbf{0}$	$\mathbf{0}$	$\mathbf{B}_{11,10}\mathbf{U}_{10}$	$\mathbf{A}_{11,11}$	$\mathbf{B}_{11,12}\mathbf{U}_{12}$
$\mathbf{0}$	$\mathbf{0}$	$\mathbf{0}$	$\mathbf{0}$	$\mathbf{0}$	$\mathbf{0}$	$\mathbf{0}$	$\mathbf{0}$	$\mathbf{0}$	$\mathbf{B}_{12,10}\mathbf{U}_{10}$	$\mathbf{B}_{12,11}\mathbf{U}_{11}$	$\mathbf{A}_{12,12}$

(4)

$\bar{\mathbf{c}}_1 = \mathbf{c}_1' - (0,0,0,\beta^{11},\beta^7,\beta) = (e_1', e_2', \beta^2, e_3', e_4', \beta)$. *Then, we solve* $\mathbf{H}_1^{\mathrm{G}}\bar{\mathbf{c}}_1^{\mathrm{T}} = (0,0,0,\beta^{11})^{\mathrm{T}}$ *and obtain* $(e_1', e_2', e_3', e_4') = (1, \beta, \beta^{10}, \beta^7)$. *Therefore,* $e_1 = e_1' = 1$, $e_2 = e_2' = \beta$, $e_3 = e_3' + \beta^{11} = \beta^{14}$, $e_4 = e_4' + \beta^7 = 0$, *and we have decoded* $\mathbf{c}_1$ *successfully.*

Note that Construction 1 is proposed based on the assumption that any node is able to communicate with all the nodes in the network; namely, the underlying DSN has a specific topology embodied in a complete graph. However, as discussed in Section I and shown in Fig. 1, practical DSNs are not necessarily constrained into any specific structures. A major reason is that nodes are typically scattered in geographically separated locations and communicate with only a few nodes nearby. Even if connections of nodes are not determined by physical locations, their logical connections can still be of any topology tailored for particular requirements from users of the services those nodes provide. Therefore, it is important to generalize our previous construction into one that fits into arbitrary topologies. In the next section, we take network topology into account and focus on constructions that are topology-adaptive.

III. Cooperative Data Protection

In this section, we first mathematically describe the EC hierarchy and its depth associated with the given DSN. EC hierarchy specifies the EC capabilities of nodes while cooperating with different sets of other nodes. We then propose a cooperation scheme where each node only cooperates with its single-hop neighbors.

A. EC Hierarchy

Denote the **EC hierarchy** of node $v_i \in V$ by a sequence $\mathbf{d}_i = (d_{i,0}, d_{i,1}, \ldots, d_{i,L_i})$, where L_i is called the **depth** of $\mathbf{d}_i$, and $d_{i,\ell}$ represents the maximum number of erased symbols v_i can recover in its codeword $\mathbf{c}_i$ from the ℓ-th level cooperation, for all $\ell \in [L_i]$. The maximum number of erased symbols v_i can recover in $\mathbf{c}_i$ locally, i.e., without communicating with neighboring nodes, is $d_{i,0}$.

For each $v_i \in V$ such that $L_i > 0$, there exist two series of sets of nodes, denoted by $\varnothing \subset \mathcal{A}_i^1 \subset \mathcal{A}_i^2 \subset \cdots \subset \mathcal{A}_i^{L_i} \subseteq V$ and $\{\mathcal{B}_i^\ell\}_{\ell=1}^{L_i}$, where $\mathcal{A}_i^\ell \cap \mathcal{B}_i^\ell = \varnothing$ for all $\ell \in [L_i]$, and a series $(\lambda_{i,\ell;\mathcal{W}})_{\varnothing \subseteq \mathcal{W} \subseteq \mathcal{B}_i^\ell}$. In the ℓ-th level cooperation, node $v_i \in V$ tolerates $\lambda_{i,\ell;\mathcal{W}}$ ($\varnothing \subseteq \mathcal{W} \subseteq \mathcal{B}_i^\ell$) erasures if all nodes in $\mathcal{A}_i^\ell \cup \mathcal{W}$ are able to decode their own messages, where the maximum value is $\lambda_{i,\ell;\mathcal{B}_i^\ell} = d_{i,\ell}$ and is reached when $\mathcal{W} = \mathcal{B}_i^\ell$; the minimum value is $\lambda_{i,\ell;\varnothing}$ and is reached when $\mathcal{W} = \varnothing$. See Fig. 2 for illustration.

We first take a look at the cooperation schemes with the EC hierarchy of depth 1. For the EC hierarchy of depth 1, $\mathcal{A}_i^1$ is always a subset of the neighbors of v_i, while $\mathcal{B}_i^1$ is the set of all nodes in $\mathcal{A}_j^1$, for all j such that v_j is in $\mathcal{A}_i^1$, except the ones in $\{v_i\} \cup \mathcal{A}_i^1$.

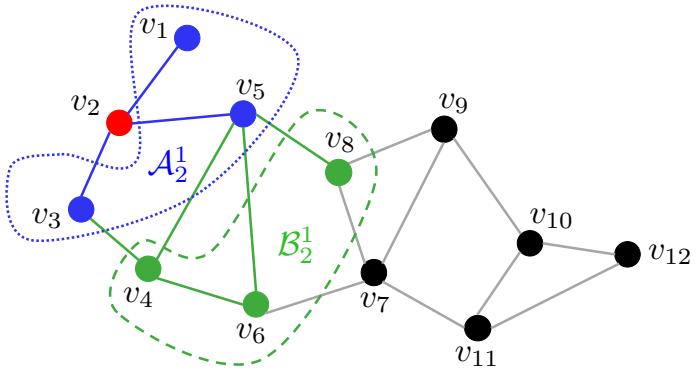


Fig. 3. DSN for Example 2. Nodes in $\mathcal{A}_2^1$ are neighbors of v_2 and are required to be locally-recoverable to remove cross parities from the parity part of $\mathbf{c}_2$. Nodes in $\mathcal{B}_2^1$ are neighbors of nodes in $\mathcal{A}_2^1$ except for v_2 and nodes in $\mathcal{A}_2^1$ themselves. For any node v_j in $\mathcal{A}_2^1$, only when all the neighbors of v_j in $\mathcal{B}_2^1$ are recovered, v_j can provide extra parity symbols to v_2.

B. Single-Level Cooperation

We now discuss the case where each node only has cooperation of depth 1. Consider a DSN represented by $G(V, E)$ that is associated with parameters $(\mathbf{n}, \mathbf{k}, \mathbf{r})$ and a class of sets $\{\mathcal{M}_i\}_{v_i \in V}$ such that $\varnothing \subset \mathcal{M}_i \subseteq \mathcal{N}_i$, for all $v_i \in V$. In Construction 2, we present a joint coding scheme where node v_i only cooperates with nodes in $\mathcal{M}_i$, for all $v_i \in V$. Heterogeneity is obviously achieved since n_i, k_i, r_i, are not required to be identical for all $v_i \in V$.

Our previous result in [1] represents a special case of Construction 2, where the motivating application was in centralized cloud storage. Construction 2 extends that work to deal with arbitrary decentralized topologies, in contrast to the tree-like topology prevalent in. centralized networks. Example 2 and Example 3 illustrate the efficacy of the proposed construction in decentralized storage.

Construction 2. *Let $G(V, E)$ represent a DSN associated with parameters $(\mathbf{n}, \mathbf{k}, \mathbf{r})$ and a local EC parameter $\boldsymbol{\delta}$, where $\mathbf{r} \succ \boldsymbol{\delta} \succeq \mathbf{0}$. Let $p = |V|$ and $\mathrm{GF}(q)$ be a Galois field of size q, where $q > \max\limits_{v_i \in V} \left(n_i + \delta_i + \sum_{v_j \in \mathcal{M}_i} \delta_j\right)$.*

For each $i \in [p]$, let $a_{i,x}$, $x \in [k_i + \delta_i]$, and $b_{i,y}$, $y \in \left[r_i + \sum_{v_j \in \mathcal{M}_i} \delta_j\right]$, be distinct elements of $\mathrm{GF}(q)$. Consider the Cauchy matrix $\mathbf{T}_i \in \mathrm{GF}(q)^{(k_i+\delta_i)\times(r_i+\sum_{v_j \in \mathcal{M}_i} \delta_j)}$ such that $\mathbf{T}_i = \mathbf{Y}(a_{i,1}, \ldots, a_{i,k_i+\delta_i}; b_{i,1}, \ldots, b_{i,r_i+\sum_{v_j \in \mathcal{M}_i} \delta_j})$. Matrix $\mathbf{G}$ in (1) is assembled as follows. For each $i \in [p]$, we obtain $\{\mathbf{B}_{i,j}\}_{v_j \in \mathcal{M}_i}$, $\mathbf{U}_i$, $\mathbf{A}_{i,i}$, according to the following partition of $\mathbf{T}_i$:

$$\mathbf{T}_i = \left[\begin{array}{c|c|c|c} \mathbf{A}_{i,i} & \mathbf{B}_{i,j_1} & \cdots & \mathbf{B}_{i,j_{|\mathcal{M}_i|}} \\ \hline \mathbf{U}_i & \multicolumn{3}{c}{\mathbf{Z}_i} \end{array}\right], \tag{5}$$

where $\mathcal{M}_i = \{v_{j_1}, v_{j_2}, \ldots, v_{j_{|\mathcal{M}_i|}}\}$, $\mathbf{A}_{i,i} \in \mathrm{GF}(q)^{k_i \times r_i}$, $\mathbf{U}_i \in \mathrm{GF}(q)^{\delta_i \times r_i}$, $\mathbf{B}_{i,j} \in \mathrm{GF}(q)^{k_i \times \delta_j}$, for $v_i \in V$ and $v_j \in \mathcal{M}_i$. Let $\mathbf{A}_{i,j} = \mathbf{B}_{i,j}\mathbf{U}_j$ if $v_j \in \mathcal{M}_i$, otherwise let it be a zero matrix.

Denote the code with generator matrix $\mathbf{G}$ by $\mathcal{C}_1$.

Theorem 1. *In a DSN with $\mathcal{C}_1$, $\mathbf{d}_i = (r_i - \delta_i, r_i + \sum_{v_j \in \mathcal{M}_i} \delta_j)$, $\mathcal{A}_i^1 = \mathcal{M}_i$, and $\mathcal{B}_i^1 = \bigcup_{v_j \in \mathcal{M}_i} (\mathcal{M}_j \setminus (\{v_i\} \cup \mathcal{M}_i))$, for all $v_i \in V$. Furthermore, the EC hierarchy associated with $d_{i,1}$ is $(\lambda_{i,1;\mathcal{W}})_{\varnothing \subseteq \mathcal{W} \subseteq \mathcal{B}_i^1}$, where $\lambda_{i,1;\mathcal{W}} = r_i + \sum_{j: v_j \in \mathcal{M}_i, (\mathcal{M}_j \setminus \{v_i\}) \subseteq (\mathcal{M}_i \cup \mathcal{W})} \delta_j$.*

Proof. It follows directly from Lemma 2 that for all $i \in [p]$, the i-th entry of the EC hierarchy at node v_i is $\mathbf{d}_i = (r_i - \delta_i, r_i + \sum_{v_j \in \mathcal{M}_i} \delta_j)$. The remaining task is to prove that $\lambda_{i,1;\mathcal{W}} = r_i + \sum_{j: v_j \in \mathcal{M}_i, (\mathcal{M}_j \setminus \{v_i\}) \subseteq (\mathcal{M}_i \cup \mathcal{W})} \delta_j$.

For all $v_i \in V$, let $\mathbf{s}_i = \sum_{v_j \in \mathcal{M}_i} \mathbf{m}_j \mathbf{B}_{j,i}$. We first notice that for any $v_i \in V$, $v_j \in \mathcal{M}_i$, if $\mathbf{m}_j$ is recoverable, then the additional cross parities $\mathbf{s}_j \mathbf{U}_j$ and the original cross parities $\mathbf{m}_j \mathbf{A}_{j,j}$ of v_j can be computed. Therefore, $\mathbf{s}_j$ can be computed, and if all the messages $\{\mathbf{m}_{j'}\}_{v_{j'} \in \mathcal{M}_j \setminus \{v_i\}}$ are further recoverable, then the cross parities $\mathbf{m}_i \mathbf{B}_{i,j}$ of v_i from v_j can be computed from $\mathbf{m}_i \mathbf{B}_{i,j} = \mathbf{s}_j - \sum_{v_{j'} \in \mathcal{M}_j \setminus \{v_i\}} \mathbf{m}_{j'} \mathbf{B}_{j',j}$.

Previous discussion implies that for any $\mathcal{W}$, $\varnothing \subseteq \mathcal{W} \subseteq \mathcal{B}_i^1$, if $(\mathcal{M}_j \setminus \{v_i\}) \subseteq (\mathcal{M}_i \cup \mathcal{W})$, then the additional δ_j cross parities $\mathbf{m}_i \mathbf{B}_{i,j}$ of $\mathbf{m}_i$ can be obtained. Therefore, $\lambda_{i,1;\mathcal{W}} = r_i + \sum_{j: v_j \in \mathcal{M}_i, (\mathcal{M}_j \setminus \{v_i\}) \subseteq (\mathcal{M}_i \cup \mathcal{W})} \delta_j$. ∎

Example 2. *Consider the DSN shown in Fig. 3. Let $\mathcal{M}_i = \mathcal{N}_i$ in Construction 2, for all $i \in [12]$. The matrix in (4) is obtained by removing all the block columns of identity surrounded by zero matrices from the generator matrix (1) of $\mathcal{C}_1$, and is referred to as the* **non-systematic component** *of the generator matrix.*

Take node v_2 as an example. Observe that $\mathcal{A}_2^1 = \mathcal{M}_2 = \{v_1, v_3, v_5\}$, $\mathcal{A}_1^1 = \mathcal{M}_1 = \{v_2\}$, $\mathcal{A}_3^1 = \mathcal{M}_3 = \{v_2, v_4\}$, and $\mathcal{A}_5^1 = \mathcal{M}_5 = \{v_2, v_4, v_6, v_8\}$. Therefore, $\mathcal{B}_2^1 = \bigcup_{j \in \{1,3,5\}} \mathcal{M}_j \setminus \{v_1, v_2, v_3, v_5\} = \{v_4, v_6, v_8\}$. Moreover, $\mathbf{d}_2 = (r_2 - \delta_2, r_2 + \sum_{j \in \{1,3,5\}} \delta_j)$, $\lambda_{2,1;\varnothing} = \lambda_{2,1;\{v_6\}} = \lambda_{2,1;\{v_8\}} = \lambda_{2,1;\{v_6,v_8\}} = r_2 + \delta_1$, $\lambda_{2,1;\{v_4\}} = \lambda_{2,1;\{v_4,v_6\}} = \lambda_{2,1;\{v_4,v_8\}} = r_2 + \delta_1 + \delta_3$, and $\lambda_{2,1;\{v_4,v_6,v_8\}} = r_2 + \delta_1 + \delta_3 + \delta_5$.

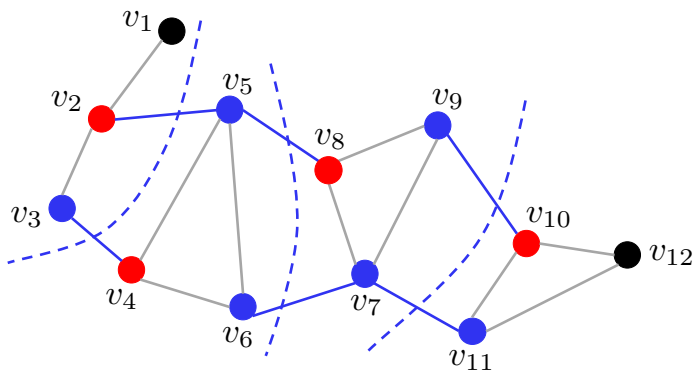


Fig. 4. The erasure pattern in Example 4. Red and non-red nodes refer to nodes where the codewords stored at them are non-locally-recoverable and locally-recoverable, respectively.

Consider the case where the 1*-st level cooperation of* v_2 *is initiated, i.e., the number of erasures lies within the interval* $[r_2 - \delta_2 + 1, r_2 + \delta_1 + \delta_3 + \delta_5]$*. Then, if* $\mathbf{m}_1, \mathbf{m}_3, \mathbf{m}_5$ *are all locally-recoverable, the cross parities* $\mathbf{m}_1\mathbf{B}_{1,2}$*,* $\mathbf{m}_3\mathbf{B}_{3,2}$*,* $\mathbf{m}_5\mathbf{B}_{5,2}$ *computed from the non-diagonal parts in the generator matrix can be subtracted from the parity part of* $\mathbf{c}_2$ *to get* $\mathbf{m}_2\mathbf{A}_{2,2}$*. Moreover, the successful decoding of* $\mathbf{m}_1$ *makes* $\mathbf{m}_2\mathbf{B}_{2,1}$ *known to* v_2*. This process provides* $(r_2 + \delta_1)$ *parities for* $\mathbf{m}_2$*, and thus allows* v_2 *to tolerate* $(r_2 + \delta_1)$ *erasures.*

In order to correct more than $(r_2+\delta_1)$ *erasures, we need extra cross parities generated from* $\mathbf{B}_{2,3}\mathbf{U}_3$ *and* $\mathbf{B}_{2,5}\mathbf{U}_5$*. However, local decoding only allows* v_3*,* v_5 *to know* $\mathbf{m}_2\mathbf{B}_{2,3} + \mathbf{m}_4\mathbf{B}_{4,3}$ *and* $\mathbf{m}_2\mathbf{B}_{2,5} + \mathbf{m}_4\mathbf{B}_{4,5} + \mathbf{m}_6\mathbf{B}_{6,5} + \mathbf{m}_8\mathbf{B}_{8,5}$*, respectively. Therefore,* v_3 *needs* $\mathbf{m}_4$ *to be recoverable to obtain the extra* δ_3 *cross parities, and* v_5 *needs* $\mathbf{m}_4$*,* $\mathbf{m}_6$*,* $\mathbf{m}_8$ *to be recoverable to obtain the extra* δ_5 *cross parities.*

As shown in Example 2, instead of presenting a rigid EC capability, our proposed scheme enables nodes to have correction of a growing number of erasures with bigger sets of neighboring nodes recovering their messages. Therefore, nodes automatically choose the shortest path to recover their messages, thus significantly increasing the average recovery speed, especially when the erasures are distributed non-uniformly and sparsely, which is important for blockchain-based DSNs [31], [32]. Moreover, nodes with higher reliabilities are utilized to help decode the data of less reliable nodes, enabling correction of erasure patterns that are not recoverable in our previous work in [1]. We show these properties in Example 3 and Example 4.

Example 3. (Faster Recovery Speed) *Consider a DSN with the cooperation scheme specified in Example 2. Suppose the time to be consumed on transferring information through the communication link* $e_{i,j}$ *is* $t_{i,j} \in \mathbb{R}^+$*, where* $t_{i,j} = t_{j,i}$ *for all* $i, j \in [12]$*,* $i \neq j$*, and* $\max\{t_{1,2}, t_{2,5}\} < (t_{2,3} + t_{3,4}) < t_{2,5} + \min\{t_{4,5}, t_{5,6}, t_{5,8}\}$*.*

Consider the case where $\mathbf{c}_2$ *at node* v_2 *has* $(r_2 + 1)$ *erasures, which implies that in addition to the case of* $\mathbf{m}_1$*,* $\mathbf{m}_3$*,* $\mathbf{m}_5$ *being obtained locally, recovering* $\mathbf{m}_4$ *is sufficient for* v_2 *to successfully obtain its message. The time consumed for decoding is* $(t_{2,3} + t_{3,4})$*. Therefore, any system using network coding with the property that a node failure is recovered through accessing more than* 4 *other nodes will need longer processing time for this case.*

Example 4. (Flexible Erasure Patterns) *Consider the DSN with the cooperation scheme specified in Example 2. Suppose* $\{\mathbf{m}_i\}_{i\notin\{2,4,8,10\}}$ *are all locally-recoverable. Then, consider the case where* $\mathbf{m}_i$ *has* $(r_i + 1)$ *erasures for* $i \in \{2, 4, 8, 10\}$*, which exemplifies a correctable erasure pattern for our proposed codes.*

The hierarchical coding scheme presented in [1] can recover from this erasure pattern only if the code used adopts a partition of all nodes into 4 *disjoint groups, each of which contains exactly a node from* $\{v_2, v_4, v_8, v_{10}\}$*, as shown in Fig. 4. Moreover, the partition of the code in [1] results in a reduction of the EC capability of the* 1*-st level cooperation at every node except for* v_1, v_{12} *because the additional information Construction 2 allows to flow through the edges marked in blue no longer exists.*

C. Recoverable Erasure Patterns

For a code specified for a DSN according to Construction 2, we next investigate the recoverable erasure patterns under the proposed EC solution. Throughout this paper, for any edge (i, j) from v_i to v_j in a directed graph $G(V, E)$, we call v_j a child of v_i, and v_i a parent of v_j.

In the DSN depicted in Fig. 5, suppose all codewords stored at black nodes are locally-recoverable; those stored at green nodes, e.g., v_i with $i \in \{6, 8, 12\}$, are recoverable by accessing their neighboring nodes in $\mathcal{A}_i^1$ only; and those in blue nodes, e.g., v_i with $i \in \{0, 2, 3, 5, 10\}$, need some nodes in $\mathcal{B}_i^1$ to be also recoverable since they need to obtain extra cross parities from at least one of their neighboring nodes in $\mathcal{A}_i^1$. As an example, assume that node v_0 needs to obtain extra parities from only one of its neighbors, say v_1. This condition requires codewords stored at $v_2, v_3, v_{13}, v_{14}, v_{15}$ all being recoverable. Since codewords in v_{13}, v_{14}, v_{15} are already locally-recoverable, this case essentially requires codewords in v_2, v_3 to be recovered.

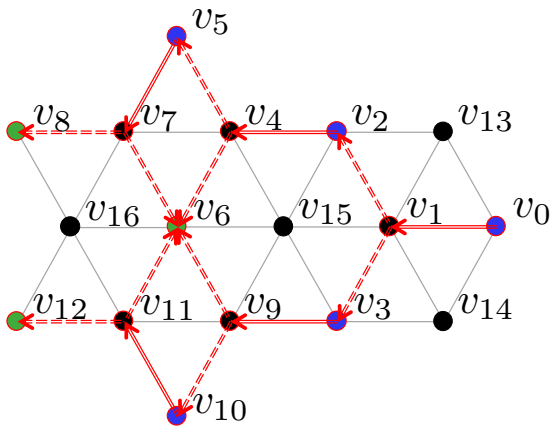


Fig. 5. Decoding graph in Definition 2. Black and non-black nodes refer to locally-recoverable and non-locally-recoverable nodes, respectively, where green nodes are recoverable without requiring any node that is not in their neighborhood to be recovered. The subgraph marked in red is a decoding graph at root node v_0. When there exists an edge pointing from v_i to v_j, v_i needs to obtain cross parities from v_j while decoding v_0, where the edges are solid if and only if v_i is non-locally-recoverable.

For simplicity, we just refer to this requirement as "v_0 needs v_2, v_3". Similarly, v_2 needs v_5, v_6, v_3 needs v_6, v_{10}, v_5 needs v_6, v_8, and v_{10} needs v_6, v_{12}. Given that codewords in v_6, v_8, v_{12} are recoverable, all the blue nodes are recoverable following the order v_5, v_{10}, v_2, v_3, v_0.

Note that in this paper, we suppose that in the protocol carrying out the decoding algorithm, each node, when receiving a request, either replies back with the required message, provided that the information gathered at this node suffices to provide the answer, or broadcasts a request to all its neighbors to ask for the information it needs. For now, we assume that nodes remain intact during decoding.

We next define the so-called **decoding graph** of each node where the codeword stored there is recoverable in a DSN. For a given node, this graph describes the aforementioned order of decoding non-locally-recoverable nodes involved in the process of decoding this particular node. Observe that connections between any two nodes having their codewords locally-recoverable are omitted for simplicity.

Definition 2. (Decoding Graph) *Let $G(V, E)$ represent a DSN with $|V| = p$ and $i \in [p]$. Let $\mathcal{T}(\mathcal{V}, \mathcal{E})$ denote a directed subgraph of G associated with v_j. For all $v_i \in \mathcal{V}$, denote the set containing all children of v_i by $\mathcal{V}_i^{\mathrm{C}}$, and that containing all parents of v_i by $\mathcal{V}_i^{\mathrm{P}}$. Suppose $v_j \in \mathcal{V}$ is the only node without parents. We call this node the **root** of $\mathcal{T}$. We call any node without children a **leaf**. Suppose then the codewords of all the leaves of $\mathcal{T}$ are not locally-recoverable, and any other $v_i \in \mathcal{V}$ satisfies one of the following conditions.*

1) *The codeword stored at v_i is locally-recoverable; $\mathcal{V}_i^{\mathrm{P}} \cup \mathcal{V}_i^{\mathrm{C}}$ consists of all the nodes in $\mathcal{M}_i$ such that codewords stored at them are not locally-recoverable and $|\mathcal{V}_i^{\mathrm{P}}| = 1$.*
2) *The codeword stored at v_i is not locally-recoverable; codewords stored at nodes in $\mathcal{V}_i^{\mathrm{P}} \cup \mathcal{V}_i^{\mathrm{C}}$ are all locally-recoverable.*

We call $\mathcal{T}$ a decoding graph at its root node v_j over $G(V, E)$.

As shown in Fig. 5, the decoding graph $\mathcal{T}$ at node v_0 is marked in red. Nodes marked in green are leaves in $\mathcal{T}$. Nodes $v_1, v_4, v_7, v_9, v_{11}$ satisfy Condition 1. Take v_1 as an example, $\mathcal{V}_1^{\mathrm{P}} = \{v_0\}$, and $\mathcal{V}_1^{\mathrm{C}} = \{v_2, v_3\}$. We know that $\mathcal{M}_1 = \{v_0, v_2, v_3, v_{13}, v_{14}, v_{15}\}$, where codewords stored at nodes in $\mathcal{V}_i^{\mathrm{P}} \cup \mathcal{V}_i^{\mathrm{C}} = \{v_0, v_2, v_3\}$ are not locally-recoverable. This local constraint enforces the node in $\mathcal{V}_1^{\mathrm{P}}$, i.e., v_0, to obtain the extra cross parities from v_1 after codewords stored at nodes in $\mathcal{V}_1^{\mathrm{C}}$ are recovered. Nodes $v_0, v_2, v_3, v_5, v_6, v_{10}, v_8, v_{12}$ satisfy Condition 2, and they are the nodes that need to recover their codewords in order that v_0 recovers its codeword.

Based on the definition of decoding graphs, Theorem 2 describes recoverable erasure patterns in a DSN.

Theorem 2. *Let $\mathcal{C}$ be a code with single-level cooperation on a DSN represented by $G(V, E)$, where $\mathcal{C}$ and all related parameters are specified according to Construction 2. Let $\mathbf{u} \in \mathbb{N}^p$ such that $\mathbf{u} \preceq \mathbf{n}$. Suppose $\mathcal{C}$ and $\mathbf{u}$ satisfy the following conditions:*

1) *Let V^{NL} represent the set that contains all the nodes v_i, $i \in [p]$ such that $u_i > r_i - \delta_i$. Let $V^{\mathrm{L}} = V \setminus V^{\mathrm{NL}}$. Then, for any $v_i \in V^{\mathrm{NL}}$, $\mathcal{M}_i \subset V^{\mathrm{L}}$.*
2) *For any $v_i \in V^{\mathrm{NL}}$, there exists a decoding graph $\mathcal{T}_i(\mathcal{V}_i, \mathcal{E}_i)$ at root v_i over G. Moreover, for any leaf v_j of $\mathcal{T}_i$, $u_j \leq r_j$; for any node $v_j \in \mathcal{V}_i \cap V^{\mathrm{NL}}$, $u_j \leq r_j + \sum_{v_k \in \mathcal{V}_j^{\mathrm{C}}} \delta_k$.*

Then, $\mathbf{u}$ is a **recoverable erasure pattern** *of $\mathcal{C}$ over $G(V, E)$.*

Proof. For any node $v_i \in \mathcal{V}^{\mathrm{NL}}$, consider the decoding graph $\mathcal{T}_i(\mathcal{V}_i, \mathcal{E}_i)$ at root v_i. Denote the number of nodes contained in V^{L} on the longest directed path connecting node v_i with a leaf in $\mathcal{T}_i$ by l_i, which is referred to as the **decoding depth** of v_i. We prove the statement "any node in G is recoverable" by mathematical induction on the decoding depth of the node.

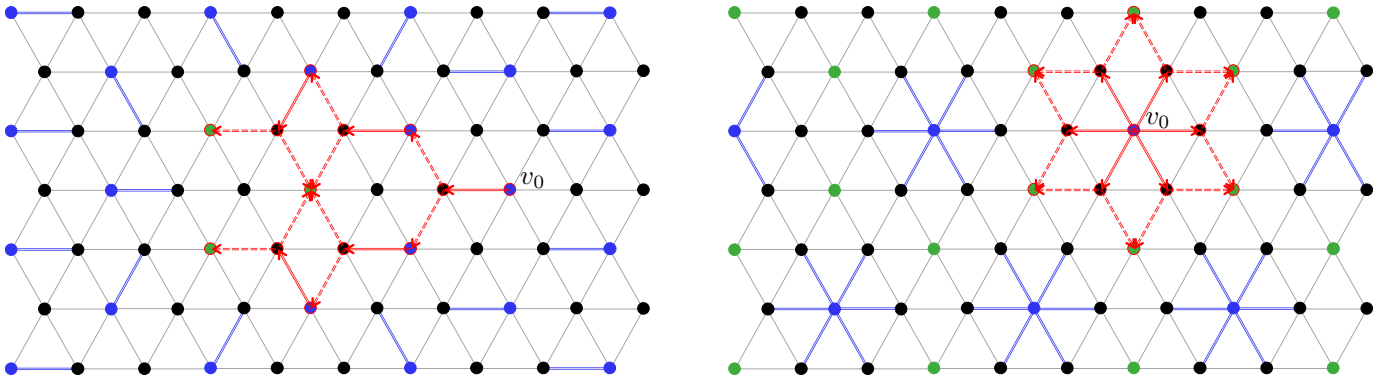


Fig. 6. DSN in Example 5. Black and non-black nodes refer to nodes that are locally-recoverable and non-locally-recoverable, respectively. The decoding graphs at v_0 are marked with color red. Any solid blue line connects a black node v_i and an non-black node v_j, where v_i is a child of v_j, and all neighbors of v_i except for v_j are children of v_i, in the decoding graph at root v_j. The blue lines uniquely describe the decoding graphs at each non-black node.

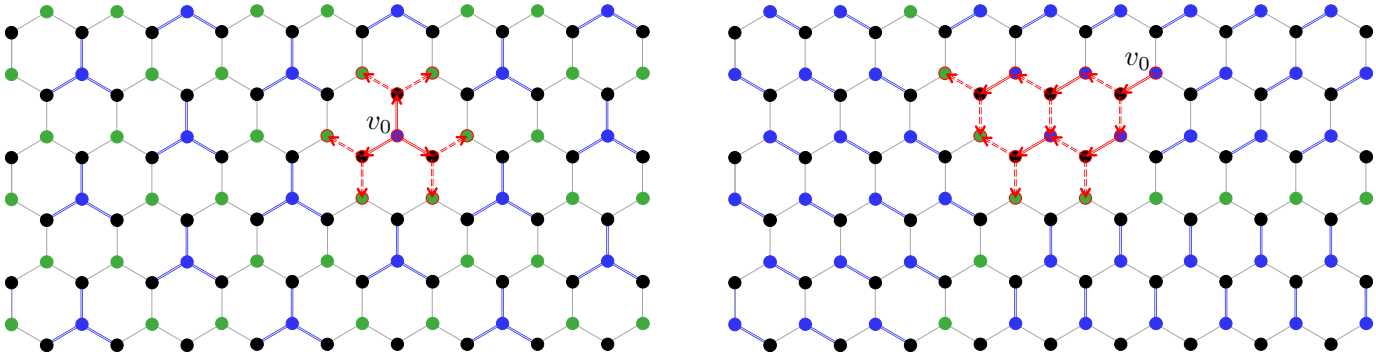


Fig. 7. DSN in Example 6. Meanings of the components of the graphs are identical to those in Fig. 6.

The decoding graph of a node with decoding depth 0 contains only the node itself. The first condition implies that all neighbors of any node that is not locally-recoverable (in $\mathcal{V}^{\mathrm{NL}}$) are locally-recoverable (in $\mathcal{V}^{\mathrm{L}}$). Therefore, any node $v_i \in \mathcal{V}^{\mathrm{NL}}$ tolerates at least r_i erasures. This means that nodes with decoding depth 0 are recoverable.

Suppose the statement is true for any node $v_j \in \mathcal{V}^{\mathrm{NL}}$ with decoding depth less than or equal to $\ell \in \mathbb{N}$. Then, for any node v_i with decoding depth $\ell+1$, let S_i denote the union of all sets $\mathcal{V}_j^{\mathrm{C}}$ such that $v_j \in \mathcal{V}_i^{\mathrm{C}}$. Since the subgraph of $\mathcal{T}_i$ rooted at any node $v_j \in S_i$ is a decoding graph of v_j with length at most ℓ, v_j is recoverable. Condition 1) in Definition 2 indicates that all neighbors of $v_j \in \mathcal{V}_i^{\mathrm{C}}$ except for v_i are recoverable and $\mathbf{m}_i\mathbf{B}_{i,j}$ is known, which provides δ_j extra parities of $\mathbf{m}_i$. Therefore, node v_i tolerates up to $r_i + \sum_{v_j \in \mathcal{V}_i^{\mathrm{C}}} \delta_j$ erasures, thus is recoverable according to Condition 2). Consequently, the statement for $\ell+1$ is also true.

By induction, the statement is true for all the nodes, and the theorem is true. ■

The following two examples illustrate Theorem 2. They follow the notation in Construction 2 and Theorem 2.

Example 5. *Fig. 6 presents two erasure patterns, $\mathbf{u}_1 = (u_{1,1}, u_{1,2}, \ldots, u_{1,p})$ (left) and $\mathbf{u}_2 = (u_{2,1}, u_{2,2}, \ldots, u_{2,p})$ (right), on the same DSN denoted by $G(V, E)$ with the EC solution characterized by $\mathcal{C}$ specified in Construction 2. Suppose there exists $\delta \in \mathbb{N}$ such that $\delta_i = \delta$ for all $i \in [p]$.*

For any $i \in [p]$, v_i is marked in black if $u_{j,i} \leq r_i - \delta$, in green if $r_i - \delta < u_{j,i} \leq r_i$, and in blue otherwise, where $j \in \{0, 1\}$. In the left panel, that specifies $\mathbf{u}_1$, any node v_i marked in blue satisfies $r_i < u_{1,i} \leq r_i + \delta$. In the right panel, that specifies $\mathbf{u}_2$, any node v_i marked in blue satisfies $r_i < u_{2,i} \leq r_i + 6\delta$.

Note that any non-black node is connected to exactly one black node by a blue edge, where the non-black node is the only parent of the black node in Definition 2. Then, for any node v_i in $G(V, E)$, there exists a decoding graph at v_i, with the leaves being all marked in green. In Fig. 6, the decoding graph at the node v_0 is marked in red on each graph of the two. Let d_i be the maximum number of erasures node v_i tolerates, for all $i \in [p]$, and $\Delta_i = d_i - r_i$. Suppose $p \to \infty$ in $G(V, E)$. Denote the average of all Δ_i's by Δ.

In the first subgraph, there will be approximately $2p/3$ nodes with any v_i of them satisfying $\Delta_i = -\delta$, and approximately $p/3$ nodes with any v_i of them satisfying $\Delta_i = \delta$. Thus, $\Delta = -\delta/3$. Similarly, in the second graph, there will be approximately $2p/3$, $2p/9$, and $p/9$ nodes with any v_i of them satisfying $\Delta_i = -\delta$, $\Delta_i = 0$, and $\Delta_i = 6\delta$, respectively. Thus, $\Delta = 0$.

Example 6. *Similar to Example 5, Fig. 7 also presents two erasure patterns on another DSN with an EC solution characterized by $\mathcal{C}$ specified in Construction 2. Suppose there exists $\delta \in \mathbb{N}$ such that $\delta_i = \delta$ for all $i \in [p]$.*

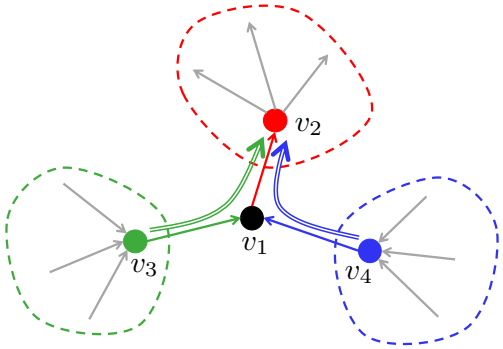


Fig. 8. Information flow in cooperative data protection. As a neighbor of v_2, v_1 helps in removing the cross parities from the parity part of $\mathbf{c}_2$. However, nodes v_3 and v_4 also indirectly help v_1 to provide extra cross parities to v_2 if they are recovered. This can be interpreted as information flow from v_3 and v_4 to v_2 through v_1.

1	2	3	4	5	6	7	8	9	10	11	12
$\mathbf{A}_{1,1}$	$\mathbf{B}_{1,2}\mathbf{U}_2$	$\mathbf{0}$	$\mathbf{0}$	$\mathbf{0}$	$\mathbf{0}$	$\mathbf{0}$	$\mathbf{0}$	$\mathbf{0}$	$\mathbf{0}$	$\mathbf{0}$	$\mathbf{0}$
$\mathbf{B}_{2,1}\mathbf{U}_1$	$\mathbf{A}_{2,2}$	$\mathbf{B}_{2,3}\mathbf{U}_3$	$\mathbf{0}$	$\mathbf{B}_{2,5}\mathbf{U}_5$	$\mathbf{0}$	$\mathbf{0}$	$\mathbf{B}_{e}\mathbf{V}_{8;2}$	$\mathbf{B}_{e}\mathbf{V}_{9;2}$	$\mathbf{B}_{d}\mathbf{V}_{10;3}$	$\mathbf{B}_{d}\mathbf{V}_{11;3}$	$\mathbf{0}$
$\mathbf{0}$	$\mathbf{B}_{3,2}\mathbf{U}_2$	$\mathbf{A}_{3,3}$	$\mathbf{B}_{3,4}\mathbf{U}_4$	$\mathbf{0}$	$\mathbf{0}$	$\mathbf{0}$	$\mathbf{B}_{e}\mathbf{V}_{8;2}$	$\mathbf{B}_{e}\mathbf{V}_{9;2}$	$\mathbf{B}_{f}\mathbf{V}_{10;3}$	$\mathbf{B}_{f}\mathbf{V}_{11;3}$	$\mathbf{0}$
$\mathbf{0}$	$\mathbf{0}$	$\mathbf{B}_{4,3}\mathbf{U}_3$	$\mathbf{A}_{4,4}$	$\mathbf{B}_{4,5}\mathbf{U}_5$	$\mathbf{B}_{4,6}\mathbf{U}_6$	$\mathbf{0}$	$\mathbf{B}_{\alpha}\mathbf{V}_{8;2}$	$\mathbf{B}_{\alpha}\mathbf{V}_{9;2}$	$\mathbf{B}_{g}\mathbf{V}_{10;2}$	$\mathbf{B}_{g}\mathbf{V}_{11;2}$	$\mathbf{0}$
$\mathbf{0}$	$\mathbf{B}_{5,2}\mathbf{U}_2$	$\mathbf{0}$	$\mathbf{B}_{5,4}\mathbf{U}_4$	$\mathbf{A}_{5,5}$	$\mathbf{B}_{5,6}\mathbf{U}_6$	$\mathbf{0}$	$\mathbf{B}_{5,8}\mathbf{U}_8$	$\mathbf{0}$	$\mathbf{0}$	$\mathbf{B}_{h}\mathbf{V}_{11;2}$	$\mathbf{B}_{h}\mathbf{V}_{12;2}$
$\mathbf{0}$	$\mathbf{0}$	$\mathbf{0}$	$\mathbf{B}_{6,4}\mathbf{U}_4$	$\mathbf{B}_{6,5}\mathbf{U}_5$	$\mathbf{A}_{6,6}$	$\mathbf{B}_{6,7}\mathbf{U}_7$	$\mathbf{B}_{\beta}\mathbf{V}_{8;2}$	$\mathbf{B}_{\beta}\mathbf{V}_{9;2}$	$\mathbf{B}_{j}\mathbf{V}_{10;2}$	$\mathbf{0}$	$\mathbf{B}_{j}\mathbf{V}_{12;2}$
$\mathbf{0}$	$\mathbf{0}$	$\mathbf{0}$	$\mathbf{0}$	$\mathbf{0}$	$\mathbf{B}_{7,6}\mathbf{U}_6$	$\mathbf{A}_{7,7}$	$\mathbf{B}_{7,8}\mathbf{U}_8$	$\mathbf{B}_{7,9}\mathbf{U}_9$	$\mathbf{B}_{i}\mathbf{V}_{10;2}$	$\mathbf{B}_{7,11}\mathbf{U}_{11}$	$\mathbf{B}_{i}\mathbf{V}_{12;2}$
$\mathbf{0}$	$\mathbf{B}_{m}\mathbf{V}_{2;2}$	$\mathbf{B}_{m}\mathbf{V}_{3;2}$	$\mathbf{B}_{y}\mathbf{V}_{4;2}$	$\mathbf{B}_{8,5}\mathbf{U}_5$	$\mathbf{B}_{y}\mathbf{V}_{6;2}$	$\mathbf{B}_{8,7}\mathbf{U}_7$	$\mathbf{A}_{8,8}$	$\mathbf{B}_{8,9}\mathbf{U}_9$	$\mathbf{B}_{n}\mathbf{V}_{10;2}$	$\mathbf{B}_{n}\mathbf{V}_{11;2}$	$\mathbf{0}$
$\mathbf{0}$	$\mathbf{B}_{o}\mathbf{V}_{2;2}$	$\mathbf{B}_{o}\mathbf{V}_{3;2}$	$\mathbf{B}_{z}\mathbf{V}_{4;2}$	$\mathbf{0}$	$\mathbf{B}_{z}\mathbf{V}_{6;2}$	$\mathbf{B}_{9,7}\mathbf{U}_7$	$\mathbf{B}_{9,8}\mathbf{U}_8$	$\mathbf{A}_{9,9}$	$\mathbf{B}_{9,10}\mathbf{U}_{10}$	$\mathbf{B}_{p}\mathbf{V}_{11;2}$	$\mathbf{B}_{p}\mathbf{V}_{12;2}$
$\mathbf{0}$	$\mathbf{B}_{q}\mathbf{V}_{2;3}$	$\mathbf{B}_{q}\mathbf{V}_{3;3}$	$\mathbf{B}_{r}\mathbf{V}_{4;2}$	$\mathbf{0}$	$\mathbf{B}_{r}\mathbf{V}_{6;3}$	$\mathbf{B}_{s}\mathbf{V}_{7;3}$	$\mathbf{B}_{s}\mathbf{V}_{8;3}$	$\mathbf{B}_{10,9}\mathbf{U}_9$	$\mathbf{A}_{10,10}$	$\mathbf{B}_{10,11}\mathbf{U}_{11}$	$\mathbf{B}_{10,12}\mathbf{U}_{12}$
$\mathbf{0}$	$\mathbf{B}_{x}\mathbf{V}_{2;3}$	$\mathbf{B}_{x}\mathbf{V}_{3;3}$	$\mathbf{B}_{t}\mathbf{V}_{4;2}$	$\mathbf{B}_{t}\mathbf{V}_{5;2}$	$\mathbf{0}$	$\mathbf{B}_{11,7}\mathbf{U}_7$	$\mathbf{B}_{u}\mathbf{V}_{8;3}$	$\mathbf{B}_{u}\mathbf{V}_{9;3}$	$\mathbf{B}_{11,10}\mathbf{U}_{10}$	$\mathbf{A}_{11,11}$	$\mathbf{B}_{11,12}\mathbf{U}_{12}$
$\mathbf{0}$	$\mathbf{0}$	$\mathbf{0}$	$\mathbf{0}$	$\mathbf{B}_{v}\mathbf{V}_{5;2}$	$\mathbf{B}_{v}\mathbf{V}_{6;3}$	$\mathbf{B}_{w}\mathbf{V}_{7;3}$	$\mathbf{0}$	$\mathbf{B}_{w}\mathbf{V}_{9;3}$	$\mathbf{B}_{12,10}\mathbf{U}_{10}$	$\mathbf{B}_{12,11}\mathbf{U}_{11}$	$\mathbf{A}_{12,12}$

(6)

For any $i \in [p]$, v_i is marked in black if $u_{j,i} \leq r_i - \delta$, in green if $r_i - \delta < u_{j,i} \leq r_i$, and in blue otherwise, where $j \in \{0, 1\}$. In the left panel, that specifies $\mathbf{u}_1$, any node v_i marked in blue satisfies $r_i < u_{1,i} \leq r_i + 3\delta$. In the right panel, that specifies $\mathbf{u}_2$, any node v_i marked in blue satisfies $r_i < u_{2,i} \leq r_i + \delta$. In Fig. 7, the decoding graph at the node v_0 is marked in red on both graphs of the two.

We follow the definitions of Δ_i's, $i \in [p]$, and Δ, stated in Example 5. In the left panel, there will be approximately $p/2$ nodes with any v_i of them satisfying $\Delta_i = -\delta$, approximately $p/3$ nodes with any v_i of them satisfying $\Delta_i = 0$, and $p/6$ nodes with any v_i of them satisfying $\Delta_i = 3\delta$. Thus, $\Delta = 0$. Similarly, in the right panel, there will be approximately $p/2$ and $p/2$ nodes with any v_i of them satisfying $\Delta_i = -\delta$ and $\Delta_i = \delta$, respectively. Thus, $\Delta = 0$.

Remark 1. (Information Flow in Coded DSN) *Note that the values of Δ_i's, $i \in [p]$, in Example 5 and Example 6 imply the unbalanced reliabilities of nodes in the coded DSN. In other words, any node (black) v_i with $\Delta_i < 0$ is of higher reliability than any node (blue) v_i with $\Delta_i > 0$. Therefore, any blue node utilizes extra information from non-black nodes in its neighborhood. The average Δ being nonnegative can be interpreted as a higher level of intrinsic information flow among nodes with different reliabilities in the coded DSN.*

For example, as shown in Fig. 8, suppose v_1 is a locally-recoverable node with neighboring nodes v_2, v_3, and v_4. If v_3 and v_4 are recoverable, then v_1 provides δ_1 extra parities to node v_2. Therefore, the information flows from v_3 and v_4 to v_2 through v_1, which is depicted in the figure.

IV. Multi-Level Cooperation

In this section, we extend the construction presented in Subsection III-B to codes with EC hierarchies of depth larger than 1. As is shown in schemes with single-level cooperation, cooperation utilizes the redundant information from nodes with fewer erasures to help in decoding of nodes that cannot be decoded locally. However, each node only obtains additional parities from its neighbors in the single-level cooperation, which immediately motivates us to explore multi-level cooperation to further improve the global EC capability of each node. Although multi-level cooperation inevitably degrades the local EC capability of each node, it enables the DSN to tolerate erasure patterns where erasures are distributed non-uniformly among the nodes, such as bursty erasures in few sparsely scattered nodes. In this section, we investigate the EC hierarchy of multi-level cooperation schemes. We first define the so-called **cooperation graphs** that describe how the nodes are coupled to cooperatively transmit information, and then prove the existence of hierarchical codes over a special class of cooperation graphs: the so-called **compatible graphs**.

A. Cooperation Graphs

Based on the aforementioned notation, for each $v_i \in V$ and $\ell \in [L_i]$, let $\mathcal{I}_i^\ell = \mathcal{A}_i^\ell \setminus \mathcal{A}_i^{\ell-1}$ (with $\mathcal{A}_i^0 = \varnothing$) and refer to it as the ℓ-th **helper** of v_i. We next define the so-called **cooperation matrix**.

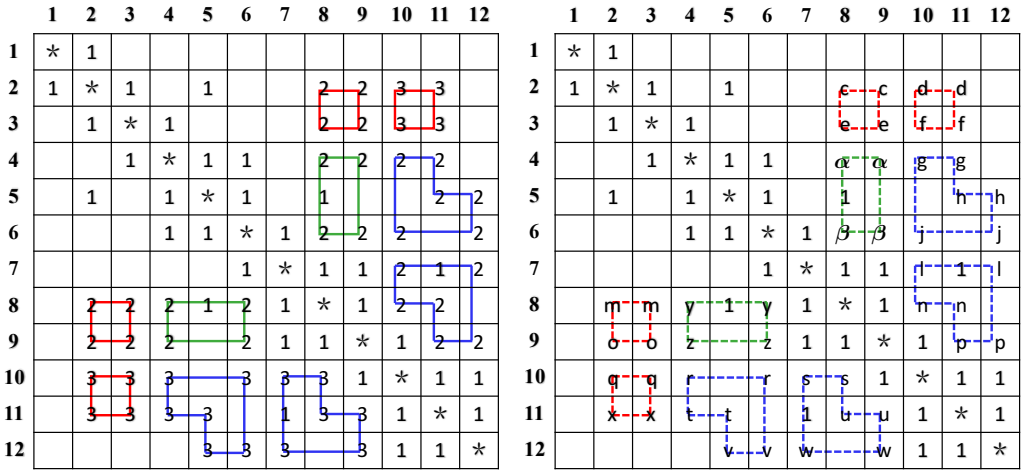


Fig. 9. Matrices $\mathbf{D}$ (left) and $\mathbf{X}$ (right) in Example 7. A numerical entry ℓ at position (i,j) in the left panel implies that v_j is adjacent to v_i in the ℓ-th level cooperation of v_i, while symbolic entries (letters) in the right panel represent the indices of the component matrices $\mathbf{A}_{i,j}$.

Definition 3. *For a joint coding scheme $\mathcal{C}$ for a DSN represented by $G(V,E)$ with $|V|=p$, the matrix $\mathbf{D}\in\mathbb{N}^{p\times p}$, in which $\mathbf{D}_{i,j}$ equals to ℓ for all $i,j\in[p]$ such that $j\in\mathcal{I}_i^\ell$, $\ell\in[L_i]$, and zero otherwise, is called the* ***cooperation matrix****.*

As an example, the cooperation matrix in Example 2 is exactly the adjacency matrix of the graph in Fig. 3. Note that cooperation graphs corresponding to some joint coding schemes must satisfy certain properties. In Subsection IV-B, we prove the existence of codes if the cooperation matrix represents a so-called **compatible graph**. Before going into details of the construction, we present an example to provide some intuition.

Example 7. *Recall the DSN in Example 2. We present a coding scheme with the cooperation matrix specified in the left panel of Fig. 9. The non-systematic part of the generator matrix is shown in (6), which is obtained through the following process:*

1) *Partition all the non-zero, non-one elements into structured groups, each of which is marked in either a rectangle or a hexagon in $\mathbf{D}$, as indicated in the left panel of Fig. 9.*
2) *Replace the endpoints of each horizontal line segment in Step 1 with $s\in S$ (S is a set of symbols), as indicated in the right panel of Fig. 9; denote the new matrix by $\mathbf{X}$.*
3) *Assign a parameter $\gamma_s\in\mathbb{N}$ to each $s\in S$, and a matrix $\mathbf{B}'_s\in\mathrm{GF}^{k_i\times\gamma_s}$ to any (i,j) such that $\mathbf{X}_{i,j}=s$.*
4) *For each $i\in[p]$, $\ell\in[L]$, let $\eta_{i;\ell}=\max_{s:k\in\mathcal{I}_i^\ell,\mathbf{X}_{k,i}=s}\gamma_s$, assign $\mathbf{V}_{i;\ell}\in\mathrm{GF}(q)^{\eta_{i;\ell}\times r_i}$ to v_i; let $\mathbf{B}_s=\left[\mathbf{B}'_s,\mathbf{0}_{\eta_{i;\ell}-\gamma_s}\right]$; compute $\mathbf{A}_{i,j}=\mathbf{B}_s\mathbf{V}_{j;\ell}$ for $s=\mathbf{X}_{i,j}$, $l=\mathbf{D}_{i,j}$.*
5) *Compute $\mathbf{A}_{i,j}$ for $\mathbf{X}_{i,j}=1$ according to Construction 2.*

Note that the colors of submatrices in (6) are consistent with the colors of cycles in Fig. 9. Let us again focus on node v_2. Let $\mathcal{I}_2^1=\{v_1,v_3,v_5\}$, $\mathcal{I}_2^2=\{v_8,v_9\}$, $\mathcal{I}_2^3=\{v_{10},v_{11}\}$. Then, $\mathcal{B}_2^1=\{v_4,v_6,v_8\}$, $\mathcal{B}_2^2=\{v_4,v_6\}$, $\mathcal{B}_2^3=\varnothing$, $d_{2,0}=r_2-\delta_2-\eta_{i;2}-\eta_{i;3}$, $d_{2,1}=r_2+\delta_1+\delta_3+\delta_5$, $d_{2,2}=d_{2,1}+\gamma_c$, $d_{2,3}=d_{2,2}+\gamma_d$. Note that for each $i\in[p]$, $s=\mathbf{X}_{i,j}$, and $l=\mathbf{D}_{i,j}$, γ_s denotes the maximum number of parity symbols v_i can obtain from v_j in the ℓ-th level cooperation, and $\eta_{i;\ell}$ represents the reduction in the value of the local erasure correction capability needed at v_i because of its ℓ-th level cooperation.

We first show that knowing $\{\mathbf{m}_j\}_{v_j\in\mathcal{A}_2^1}$ is sufficient for removing $\mathbf{s}_2=\sum_{j\in\mathcal{I}_2^1}\mathbf{m}_j\mathbf{B}_{j,2}\mathbf{U}_2+\sum_{\ell=2}^3\sum_{j\in\mathcal{I}_2^\ell}\mathbf{m}_j\mathbf{B}_{\mathbf{X}_{j,2}}\mathbf{V}_{2;\ell}$ from the parity part of $\mathbf{c}_2$. Note that if the rows of $\mathbf{A}_{i,i}$, $\mathbf{U}_i$, and $\{\mathbf{V}_{i;\ell}\}_{\ell\in\{2,3\}}$ are linearly independent, then for all ℓ, $\sum_{j\in\mathcal{I}_i^\ell}\mathbf{m}_j\mathbf{B}_{\mathbf{X}_{j,i}}$ is recoverable if $\mathbf{m}_i$ is recoverable. In our example, this means that $\{\mathbf{m}_j\mathbf{B}_{j,2}\}_{j=1,3,5}$, $\mathbf{m}_8\mathbf{B}_m+\mathbf{m}_9\mathbf{B}_o$, $\mathbf{m}_{10}\mathbf{B}_o+\mathbf{m}_{11}\mathbf{B}_x$ are known, which means $\mathbf{s}_2$ is also known. Therefore, $\mathbf{s}_2$ is removed from the parity part of $\mathbf{c}_2$ through the 1-st level cooperation. We next show that additional parities are obtained through ℓ-th level cooperations with $\ell\in\{2,3\}$.

In the 2-nd level cooperation, $\mathbf{m}_8,\mathbf{m}_9$ are known. Therefore, $\mathbf{m}_2\mathbf{B}_c+\mathbf{m}_3\mathbf{B}_e+\mathbf{m}_4\mathbf{B}_\alpha+\mathbf{m}_6\mathbf{B}_\beta$ is also known. We remove $\mathbf{m}_3\mathbf{B}_e$, that is obtained via v_3, from the parity part of $\mathbf{c}_2$. In order to obtain the γ_c parities from $\mathbf{m}_2\mathbf{B}_c$, one needs $\mathbf{m}_4,\mathbf{m}_6$ to be recoverable. Therefore, $\mathcal{B}_2^2=\{v_4,v_6\}$, $d_{2,2}=d_{2,1}+\gamma_c$, $\lambda_{2,2;\varnothing}=d_{2,1}$.

The cooperation matrix adopts a partition of non-zero, non-one elements into groups where each of them forms a cycle (see Example 7). Suppose there are T cycles. Represent each cycle with index $t\in[T]$ by a tuple $C_t=(X_t,Y_t,\{X_{t;j}\}_{j\in Y_t},\{Y_{t;i}\}_{i\in X_t},g_t,(\ell_{t;j})_{j\in Y_t})$, where X_t and Y_t denote the sets containing indices of the rows and the columns of the cycle, respectively. Let $X_{t;j}=\{i_1,i_2\}$ for $j\in Y_t$, where $(i_1,j),(i_2,j)$ are the vertices of the cycle C_t with column index j. Let $Y_{t;i}=\{j_1,j_2\}$ for $i\in X_t$, where $(i,j_1),(i,j_2)$ are the vertices of the cycle C_t with row index i. Let g_t denote a group number assigned to the cycle C_t, which will be explained shortly. Observe that any two vertices of a cycle that share the same column have the same cooperation level. Let $\ell_{t;j}$ denote the number representing the cooperation level assigned to the vertices $(i_1,j),(i_2,j)$ of the cycle C_t where $X_{t;j}=\{i_1,i_2\}$. Suppose values in $(g_t)_{t\in[T]}$ span all the values in $[A]$, for some $A\in\mathbb{N}$. For any $g\in[A]$, denote the set containing all t such that $g_t=g$ by T_g.

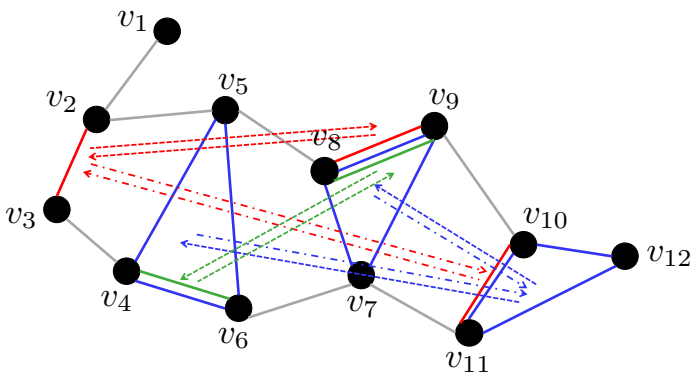


Fig. 10. Cooperation graph of Example 7. Dashed directed edges are used for cooperation level 2, and dash-dotted directed edges are used for cooperation level 3.

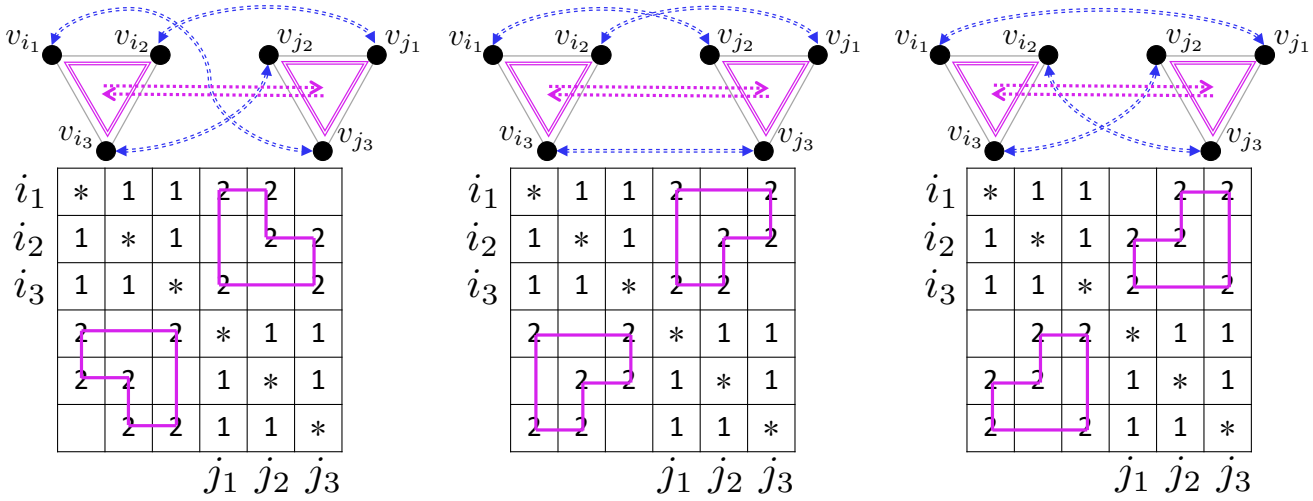


Fig. 11. Possible local matching graphs and their corresponding local cooperation matrices contained in a multi-level cooperation graph between 6 nodes.

For example, let $t = 1$ for the blue cycle at the bottom left panel of the matrices in Fig. 9. Then, the cycle C_1 is represented by $(\{10, 11, 12\}, \{4, 5, 6\}, \{X_{1;j}\}_{j=4}^{6}, \{Y_{1;i}\}_{i=10}^{12}, 1, (\ell_{1;j})_{j=4}^{6})$, where $X_{1;4} = \{10, 11\}$, $X_{1;5} = \{11, 12\}$, $X_{1;6} = \{10, 12\}$, $Y_{1;10} = \{4, 6\}$, $Y_{1;11} = \{4, 5\}$, $Y_{1;12} = \{5, 6\}$, and $\ell_{1;4} = \ell_{1;5} = \ell_{1;6} = 3$.

Observe that cycle C_t, $t \in [T]$, in Fig. 9 essentially represents a cycle in the complementary graph[2]. $\bar{G}$ of G on V, since each vertex (i, j) on the cycle implies that $\mathbf{D}_{i,j} \neq 1$, i.e., there is no edge connecting v_i and v_j in G, and there is an edge (i, j) in the complementary graph $\bar{G}$. Cycle C_t can also be interpreted as a pair of non-adjacent edges or non-overlapping triangles in G with vertices from X_t and Y_t. We mark X_t, Y_t, add an edge with arrow and the label g_t that points from X_t to Y_t for each $t \in [T]$, and obtain the so-called **cooperation graph**[3]. The cooperation graph for the coding scheme in Example 7 is shown in Fig. 10.

From the aforementioned description, a cooperation graph does not necessarily lead to a unique cooperation matrix, since the latter requires not only to further specify the associated set of cooperation levels, but also to identify the associated local matching graph, to be defined soon, for each cycle C_t if X_t has more than two nodes. For example, Fig. 11 presents three out of a total of six possible ways to specify $\{X_{t;j}\}_{j\in Y_t}$ and $\{Y_{t;i}\}_{i\in X_t}$ for a cooperation cycle C_t with $X_t = \{i_1, i_2, i_3\}$ and $Y_t = \{j_1, j_2, j_3\}$. As indicated by Fig. 11, each specified cycle of the three is uniquely represented by the set $\{(i, j)\}_{i\in X_t, Y_t\setminus Y_{t;i}=\{j\}}$ of edges that are not on the cycle. In these three graphs, if a double-dashed blue line with bidirectional arrows connects node v_{i_x} to node v_{j_y}, this means that v_{i_x} cooperates with the two nodes in $Y_t \setminus \{v_{j_y}\}$ in the cooperation involving vertices on the two triangles containing v_{j_x}, v_{i_y}, respectively. We refer to the resulting graph as a **matching graph** corresponding to a cycle. If there is more than one cycle involved in the matching graph, we call that graph a **local matching graph**. If cycles in the local matching graph are all the cycles of a cycle group, we call that graph an **isolated local matching graph** and will discuss it in detail in Subsection IV-B.

Observe that although in Example 7, the cooperation levels $(\ell_{t;j})_{t\in[T],j\in Y_t}$ specified for all the nodes on any cycle C_t,

[2]The complementary graph of a graph $G(V, E)$ consists of all nodes in V and all edges that are not in E.

[3]Note that there are two types of edges in the graph. The edges of one type connect nodes that are directly connected in their 1-st level cooperation, and these are solid edges in the graph. The edges of the other type point between two groups of nodes (edges or triangles) that are adjacent in their higher level cooperation, and these are dashed arrows in the graph. For simplicity, "connected" here is used with the meaning of "adjacent".

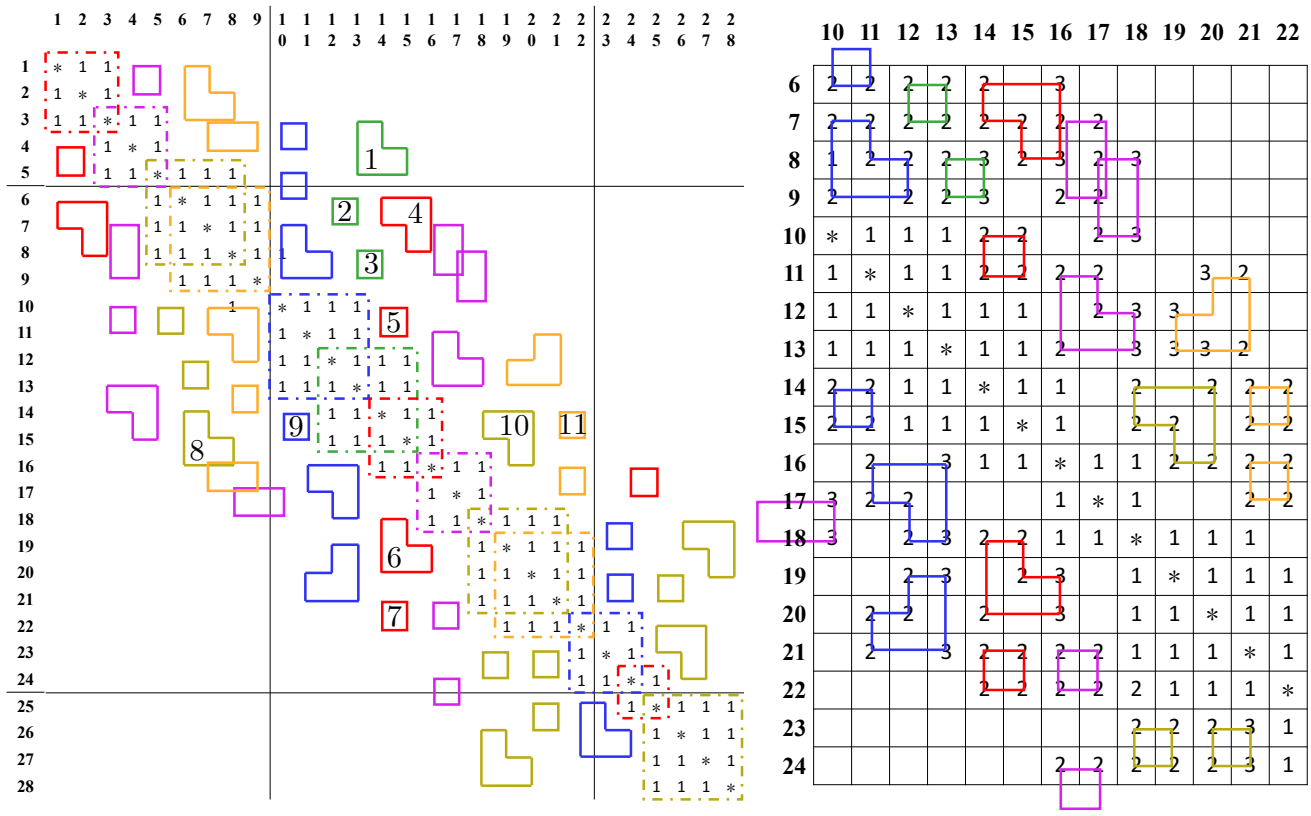


Fig. 12. Cycles and the assignment for part of the cooperation matrix on the compatible graph of a symmetric cooperation.

$t \in [T]$, are identical, this case is not a necessary condition. We present an example in Example 8, in which cooperation levels for nodes on the same cycle can be different. This example provides intuition both in deciding conditions that ensure a graph to be a cooperation graph, and in how to assign cooperation levels to such a cooperation graph if it exists.

In Subsection IV-B, we introduce the method of assigning cooperation levels over a given cooperation graph to obtain a so-called **compatible graph**. The algorithm to find a cooperation graph over a DSN $G(V, E)$ with a given topology is described in Subsection V-A.

Example 8. *The left panel of Fig. 12 presents the cycle representation of a subgraph of a compatible graph on a DSN. Denote nodes associated with the left-most column to the right-most column by v_1 to v_{28} in order, and let Fig. 13 represent the subgraph containing nodes $\{v_i\}_{5 \le i \le 22}$ of the cooperation graph. The right panel of Fig. 12 denotes the cooperation matrix of $\{v_i\}_{10 \le i \le 22}$.*

Note that some sub-matrices of the cooperation matrix are marked in dashed colored rectangles; these sub-matrices are all square matrices and have all non-diagonal entries being ones. For any such rectangle, there are cycles marked in the same color (as the rectangle) that are totally contained within the columns spanned by this rectangle; these cycles are assigned a unique group number to form a group as specified in the previous subsection. In Fig. 13, instead of writing the group number assigned to each cycle, we mark the arrow connecting nodes representing the row and column indices of the cycle with a specified color for simplicity. Moreover, each one of those dashed rectangles corresponds to a maximum clique in $G(V, E)$ that denotes the DSN.

One can easily observe that cooperation levels assigned to entries in different columns within the same cycle are not always identical. Cooperation levels assigned to two nodes within the same column are identical if and only if they are on the same cycle or they are on different cycles from the same group.

Given all the aforementioned conditions, repeat steps 2)–5) specified in Example 7 to obtain a generator matrix of a cooperative coding scheme on the DSN in this example (Example 8). Then, for any node, the cross parities resulting from each cycle group can be derived from accessing other nodes in the maximum clique that contains this group. That is to say, by communicating with all the single-level neighbors, the cross parities for each cooperation level of any node $v_i \in V$ are computable and can then be subtracted from the parity part of codeword $\mathbf{c}_i$.

Take node v_{14} as an example. The column representing v_{14} intersects with green cycles C_1 and C_3, and red cycles C_4, C_5, C_6, and C_7, corresponding to the 3-rd and the 2-nd level cooperation, respectively. All the nodes in the green clique $\{v_{12}, v_{13}, v_{14}, v_{15}\}$ except for v_{14} itself are locally-recoverable. Thus, their cross parities, resulting from the cooperation the green cycles represent, are computable, and they sum up to the 3-rd level cross parity of $\mathbf{c}_{14}$. Similarly, the 2-nd level cross parity of $\mathbf{c}_{14}$ can also be derived if the other two nodes in the red clique $\{v_{14}, v_{15}, v_{16}\}$ are locally-recoverable.

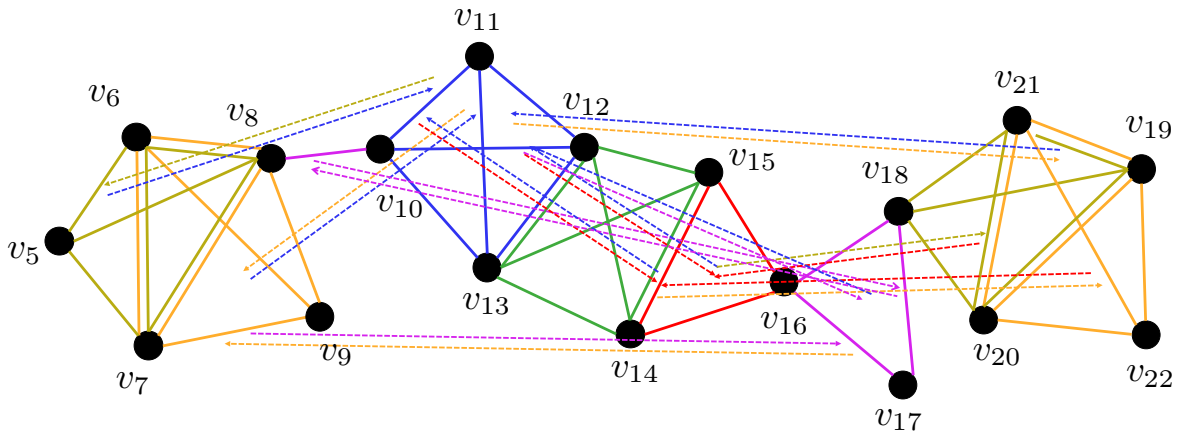


Fig. 13. Cooperation graph of Example 8. For each node, all maximum cliques containing it are marked with different colors. For any dashed arrow pointing from an edge (or a triangle) to another edge (or another triangle), with the color identical to that of the maximum clique containing the latter one: it represents a cycle in the cooperation graph that is contained in the columns spanned by this maximum clique.

More details, including the code construction, are given in Subsection IV-B and Subsection V-A.

Moreover, although Example 7 has a topologically symmetric cooperation graph and also a topologically symmetric compatible graph, it is not necessary in principle to constrain them to be symmetric. In the case where asymmetric cooperation is allowed, the basic components of the cooperation graph are edges instead of cycles, which allows more flexibility in choosing the cooperation graph. However, this asymmetry increases the complexity of defining the decoding graph for a node. Therefore, for simplicity, we only discuss topologically symmetric cooperations in this paper.

B. Construction over Compatible Graphs

We have defined the notion of cooperation graphs in Section IV-A. Observe that the cooperation graphs shown in Fig. 10 and Fig. 13 satisfy a set of conditions that define the so-called **compatible graph**. We show in Theorem 3 the existence of a hierarchical coding scheme with cooperation graph $\mathcal{G}$ if $\mathcal{G}$ is a compatible graph. The coding scheme is presented in Construction 3.

Definition 4. *For any graph $G(V,E)$ with $|V|=p$, a subgraph $G'(V',E')$ is called a **maximum clique** of G if any two nodes in V' are connected, and there does not exist any node in $V\setminus V'$ that is connected to all nodes in V'. The set of all maximum cliques of G is referred to as the **collection of maximum cliques** over G and is denoted by $\mathcal{S}(V,E)$. Each maximum clique in $\mathcal{S}$ is represented by a subset S of $[p]$, where S consists of the indices of all nodes in the maximum clique.*

Table II summarizes some notation associated with cooperation graphs that are used throughout the remainder of the paper. Take the DSN and its cooperation matrix shown in Fig. 12 as an example. Observe that the green cycles in the columns spanned by the maximum clique $\{12,13,14,15\}$ are indexed by 1, 2, and 3, and the red cycles in the columns spanned by the maximum clique $\{14,15,16\}$ are indexed by 4, 5, 6, and 7. These green and red cycles have group numbers 1 and 2, respectively. Suppose those cycles corresponding to the 2-nd level cooperation of v_{14} with top edges in the row representing v_{14} are labeled with 8, 9, 10, and 11. Note that these cycles and cycles C_4, C_5, C_6, and C_7 are symmetric with respect to the diagonal. Then, $T_1=\{1,2,3\}$, $T_2=\{4,5,6,7\}$; $A_{14}=\{1,2\}$; $S(1)=\{12,13,14,15\}$, $S(2)=\{14,15,16\}$; $U_{14;1}=V_{14;3}=\{3,4,8,9\}$; $U_{14;2}=V_{14;2}=\{6,7,10,11,18,20,21,22\}$; $R_{14;2}=\{4,5,6,7\}$; $T_{14;2}=\{8,9,10,11\}$; $\ell_{5;14}=2$; $\mathcal{M}_{14}=\mathcal{N}_{14}=\{v_{12},v_{13},v_{15},v_{16}\}$. Definition 5 formally defines the sufficient conditions that result in a compatible graph, which were discussed informally in Example 8. Note that this definition of compatible graphs is more general than that presented in the short version of the paper [2], since the cooperation levels of nodes on different columns of cycles are allowed to be different here.

Definition 5. *Let $\mathcal{G}$ be a cooperation graph on $G(V,E)$, where $\mathcal{G}$ is represented by $\{C_t=(X_t,Y_t,\{X_{t;j}\}_{j\in Y_t},\{Y_{t;i}\}_{i\in X_t},g_t,(\ell_{t;j})_{j\in Y_t})\}_{t\in[T]}$. Suppose node $v_i\in V$ has L_i cooperation levels. We call $\mathcal{G}$ a **compatible graph** on G if the following conditions are satisfied:*

1) *For any $v_i\in V$, $\mathcal{M}_i\subseteq\mathcal{N}_i$.*
2) *All cycles C_t with $t\in[T]$ are disjoint.*
3) *For any $g\in[A]$, there exists a maximum clique $S(g)\in\mathcal{S}(V,E)$ such that for all $t\in T_g$, $Y_t\subseteq S(g)$.*
4) *For each $v_i\in V$, $\ell\in[L_i]$, there exists a unique $g\in A_i$, such that $V_{i;\ell}=U_{i;g}$; denote g by $g(i;\ell)$.*

Construction 3. *Let $G(V,E)$ represent a DSN with parameters $(\mathbf{n},\mathbf{k},\mathbf{r})$. Suppose $\mathcal{G}$ is a compatible graph on G, with parameters $\{C_t=(X_t,Y_t,\{X_{t;j}\}_{j\in Y_t},\{Y_{t;i}\}_{i\in X_t},g_t,(\ell_{t;j})_{j\in Y_t})\}_{t\in[T]}$. Suppose node $v_i\in V$ has L_i cooperation levels.*

Let $\boldsymbol{\delta}$ be the 1-st level cooperation parameter. For any $v_i\in V$ and $g\in T_{i;\ell}$, assign a cooperation parameter $\gamma_{i;t}\in\mathbb{N}$ to the cooperation between node v_i and nodes in $Y_{t;i}$. Let $\eta_{j;\ell}=\max_{i\in V_{j;\ell}}\gamma_{i;t}$, for $\ell\in[L_i]$.

TABLE II
NOTATION ASSOCIATED WITH COOPERATION GRAPHS.

Notation	Physical Interpretation
A	The total number of different cycle groups
T	The total number of different cycles
T_g	The set consisting of indices of cycles with group number g
A_i	The set of group numbers of those cycle groups that intersect with the column representing v_i
$S(g)$	The set consisting of vertices of the maximum clique that contains all columns spanned by cycles in group g
$U_{j;g}$	The intersection of all cycles contained in group g with the column representing v_j
$R_{j;\ell}$	The set consisting of indices of cycles that intersect with the column representing node v_j at its ℓ-th level cooperation
$V_{j;\ell}$	The intersection of all cycles contained in $R_{j;\ell}$ with the column representing v_j
$T_{i;\ell}$	The set consisting of indices of cycles that intersect with the row representing node v_i at its ℓ-th level cooperation (cycles with labels in $R_{j;\ell}$ and $T_{i;\ell}$ are symmetric with respective to the diagonal)
$\ell_{t;j}$	The cooperation level of node v_j in cycle C_t
$\gamma_{i;t}$	The maximum number of parity symbols that nodes in cycle C_t can provide to node v_i
$\mathcal{M}_i$	The set of nodes in the 1-st level cooperation graph of v_i
$\mathcal{N}_i$	The set of nodes in the neighborhood of v_i

Let $u_i = k_i + \delta_i + \sum_{\ell=2}^{L_i} \eta_{i;\ell}$, $v_i = r_i + \sum_{v_j \in \mathcal{M}_i} \delta_j + \sum_{2 \le \ell \le L_i, t \in T_{i;\ell}} \gamma_{i;t}$, *for* $i \in [p]$. *For each* $i \in [p]$, *let* $a_{i,s}$, $s \in [u_i]$, *and* $b_{i,t}$, $t \in [v_i]$, *be distinct elements of* $\mathrm{GF}(q)$, *where* $q \ge \max_{i\in[p]}\{u_i + v_i\}$.

Matrix $\mathbf{G}$ *in (1) is assembled as follows. Consider the Cauchy matrix* $\mathbf{T}_i$ *on* $\mathrm{GF}(q)^{u_i \times v_i}$ *such that* $\mathbf{T}_i = \mathbf{Y}(a_{i,1}, \ldots, a_{i,u_i}; b_{i,1}, \ldots, b_{i,v_i})$, *for* $i \in [p]$. *Then, we obtain* $\mathbf{A}_{i,i}$, $\mathbf{B}_{i,j}$, $\mathbf{E}_{i;\ell}$, $\mathbf{U}_i$, $\mathbf{V}_{i;\ell}$, *for* $i \in [p]$, $j \in [p] \setminus \{i\}$, $\ell \in [L_i]$, *according to the following partition of* $\mathbf{T}_i$*:*

$$\mathbf{T}_i = \left[\begin{array}{c|c|c|c|c} \mathbf{A}_{i,i} & \mathbf{B}_i & \mathbf{E}_{i;2} & \cdots & \mathbf{E}_{i;L_i} \\ \hline \mathbf{U}_i & \multicolumn{4}{c}{\multirow{4}{*}{$\mathbf{Z}_i$}} \\ \cline{1-1} \mathbf{V}_{i;2} & & & & \\ \cline{1-1} \vdots & & & & \\ \cline{1-1} \mathbf{V}_{i;L_i} & & & & \end{array}\right], \tag{7}$$

$$\text{where} \quad \mathbf{B}_i = \left[\begin{array}{c|c|c} \mathbf{B}_{i,j_1} & \cdots & \mathbf{B}_{i,j_{|\mathcal{M}_i|}} \end{array}\right], \tag{8}$$

$$\text{and} \quad \mathbf{E}_{i;\ell} = \left[\begin{array}{c|c|c} \mathbf{E}_{i;\ell;t_1} & \cdots & \mathbf{E}_{i;\ell;t_{|B_{i;\ell}|}} \end{array}\right], \tag{9}$$

such that $\mathcal{M}_i = \{v_{j_1}, v_{j_2}, \ldots, v_{j_{|\mathcal{M}_i|}}\}$, $T_{i;\ell} = \{t_1, t_2, \ldots, t_{|T_{i;\ell}|}\}$, $\mathbf{A}_{i,i} \in \mathrm{GF}(q)^{k_i \times r_i}$, $\mathbf{U}_i \in \mathrm{GF}(q)^{\delta_i \times r_i}$, $\mathbf{V}_{i;\ell} \in \mathrm{GF}(q)^{\eta_{i;\ell} \times r_i}$, $\mathbf{B}_{i,j} \in \mathrm{GF}(q)^{k_i \times \delta_j}$ *for all* $v_j \in \mathcal{M}_i^1$, *and* $\mathbf{E}_{i;\ell;t} \in \mathrm{GF}(q)^{k_i \times \gamma_{i;t}}$. *Let* $\mathbf{B}_{i,j} = \left[\mathbf{E}_{i;\ell;t}, \mathbf{0}_{k_i \times (\eta_{j;\ell} - \gamma_{i;t})}\right]$, *and* $\mathbf{A}_{i,j} = \mathbf{B}_{i,j}\mathbf{V}_{j;\ell}$, *for all* $j \in Y_{t;i}$, $t \in T_{i;\ell}$. *Let* $\mathbf{A}_{i,j} = \mathbf{B}_{i,j}\mathbf{U}_j$, *for* $v_j \in \mathcal{M}_i$; *otherwise* $\mathbf{A}_{i,j} = \mathbf{0}_{k_i \times r_i}$. *Substitute the components of* $\mathbf{G}$ *in (1).*

Let $\mathcal{C}_2$ *represent the code with generator matrix* $\mathbf{G}$.

Theorem 3. *The code* $\mathcal{C}_2$ *has EC hierarchies* $\mathbf{d}_i = (d_{i,0}, d_{i,1}, \ldots, d_{i,L_i})$, *for all* $v_i \in V$, *where* $d_{i,0} = r_i - \delta_i - \sum_{\ell=2}^{L_i} \eta_{i;\ell}$, $d_{i,1} = r_i + \sum_{v_j \in \mathcal{M}_i} \delta_j$, *and* $d_{i,\ell} = r_i + \sum_{v_j \in \mathcal{M}_i} \delta_j + \sum_{2 \le \ell' \le \ell, t \in T_{i;\ell'}} \gamma_{i;t}$. *Moreover,* $\mathcal{I}_i^1 = \mathcal{M}_i$, $\mathcal{B}_i^1 = \bigcup_{v_j \in \mathcal{M}_i} (\mathcal{M}_j \setminus (\{v_i\} \cup \mathcal{M}_i))$. *For* $2 \le \ell \le L_i$, $\mathcal{I}_i^\ell = \bigcup_{t \in R_{i;\ell}} \{v_j : j \in X_{t;i}\} = \{v_j : j \in V_{i;\ell}\}$, $\mathcal{B}_i^\ell = \bigcup_{v_j \in \mathcal{I}_i^\ell} \left(\mathcal{I}_j^\ell \setminus (\{v_i\} \cup \mathcal{A}_i^\ell)\right)$ *(recall* $\mathcal{A}_i^\ell = \bigcup_{\ell' \le l} \mathcal{I}_i^{\ell'}$*),* $\lambda_{i,\ell;\mathcal{W}} = r_i + \sum_{j: v_j \in \mathcal{M}_i, (\mathcal{M}_j \setminus \{v_i\}) \subseteq (\mathcal{M}_i \cup \mathcal{W})} \delta_j + \sum_{\substack{(i,t): 2 \le \ell' \le \ell, t \in T_{i,\ell}, Y_{t;i} = \{j, j'\}, \\ \mathcal{I}_j^{\ell_{t;j}} \setminus \mathcal{A}_i^{\ell'} \subseteq (\{v_i\} \cup \mathcal{W}) \text{ or } \mathcal{I}_{j'}^{\ell_{t;j'}} \setminus \mathcal{A}_i^{\ell'} \subseteq (\{v_i\} \cup \mathcal{W})}} \gamma_{i;t}$, $\varnothing \subseteq \mathcal{W} \subseteq \mathcal{B}_i^\ell$.

Proof. For any node $v_j \in V$, denote the cross parities of v_j due to cooperation with nodes in $\mathcal{I}_j^\ell$ by $\mathbf{s}_{j;\ell}$, $\ell \in [L_j]$. The cross parities are given by the following equation:

$$\mathbf{s}_{j;\ell} = \begin{cases} \sum_{v_k \in \mathcal{M}_j} \mathbf{m}_k \mathbf{B}_{k,j}, & \ell = 1, \\ \sum_{k \in V_{j;\ell}} \mathbf{m}_k \mathbf{B}_{k,j}, & 2 \le \ell \le L_j. \end{cases} \tag{10}$$

Thus, the codeword stored at $v_j \in V$ can be expressed in the following form:

$$\begin{aligned} \mathbf{c}_j &= \mathbf{m}_j \mathbf{A}_{j,j} + \sum_{v_k \in \mathcal{M}_j} \mathbf{m}_k \mathbf{B}_{k,j} \mathbf{U}_j + \sum_{\ell=2}^{L_j} \sum_{k \in V_{j;\ell}} \mathbf{m}_k \mathbf{B}_{k,j} \mathbf{V}_{j;\ell} \\ &= \mathbf{m}_j \mathbf{A}_{j,j} + \mathbf{s}_{j;1} \mathbf{U}_j + \sum\nolimits_{\ell=2}^{L_j} \mathbf{s}_{j;\ell} \mathbf{V}_{j;\ell}. \end{aligned} \tag{11}$$

Provided that the rows of $\mathbf{A}_{j,j}$, $\mathbf{U}_j$, and $\{\mathbf{V}_{j;\ell}\}_{\ell=2}^{L_j}$ are linearly independent, $\mathbf{m}_j$ and $\{\mathbf{s}_{j;\ell}\}_{\ell \in [L_j]}$ are all computable if $\mathbf{c}_j$ is locally-recoverable.

We first show that by communicating with all the neighboring nodes in the 1-st level cooperation, the cross parities $\{\mathbf{s}_{i;\ell}\}_{\ell \in [L_i]}$ of any node $v_i \in V$ can be computed and removed from the parity part of the codeword stored at this node if all its neighbors

are locally-recoverable. Under this condition on the neighbors of v_i, calculating $\mathbf{s}_{i;1}$ is trivial. Next, we prove for $2 \leq \ell \leq L_i$ that $\{\mathbf{s}_{i;\ell}\}$ can also be computed.

Condition 4) in Definition 5 indicates that there exists a unique $g = g(i;\ell) \in A_i$, such that the following equation holds:

$$\mathbf{s}_{i;\ell} = \sum\nolimits_{j \in U_{i;g}} \mathbf{m}_j \mathbf{B}_{j,i}. \tag{12}$$

Moreover, Condition 3) guarantees the existence of a maximum clique $S(g) \in \mathcal{S}(V,E)$ such that for all $t \in T_g$, $Y_t \subseteq S(g)$. Let $\beta_{i;g} = \max_{\{(i,\ell):g(i;\ell)=g\}} \eta_{i;\ell}$, and $\mathbf{u}_{i;\ell} = \left[\mathbf{s}_{i;\ell}, \mathbf{0}_{\beta_{i;g}-\eta_{i;\ell}}\right]$, for all $i \in [p]$, $\ell \in [L_i]$. We now consider:

$$\begin{aligned}
\sum_{(i,\ell):g(i;\ell)=g} \mathbf{u}_{i;\ell} &= \sum_{t\in T_g, i\in X_t, j\in Y_{t;i}} \left[\mathbf{m}_i \mathbf{B}_{i,j}, \mathbf{0}_{\beta_{i;g}-\eta_{i;\ell_{t;i}}}\right] \\
&= \sum_{t\in T_g, i\in X_t, j\in Y_{t;i}} \left[\mathbf{m}_i \mathbf{E}_{i;\ell_{t;i};t}, \mathbf{0}_{\beta_{i;g}-\gamma_{i;t}}\right] \\
&= \sum_{t\in T_g, i\in X_t} \mathbf{0}_{\beta_{i;g}} = \mathbf{0}_{\beta_{i;g}}.
\end{aligned}$$

It follows that $\mathbf{s}_{i;\ell}$ can be derived from $\mathbf{u}_{i;\ell}$ if all $\mathbf{s}_{j;\ell'}$ such that $g(j;\ell') = g$ are known. Condition 3) in Definition 5 implies that all these j's belong to $S(g)$, and the set of nodes indexed by $S(g)$ is a subset of $\mathcal{M}_i$, which means that all the aforementioned $\mathbf{s}_{j;\ell'}$'s are computable given that the neighbors of v_i are locally-recoverable.

We have proved that all the ℓ-th level cross parities, $\ell \in [L_i]$, of any node $v_i \in V$ can be computed if the neighboring nodes are locally-recoverable. Now, we move forward to calculate the EC hierarchies of each node. Observe that the local and the 1-st level cooperation erasure correction capabilities are proved the same way they are proved for Theorem 1. Thus, we only consider cases where $2 \leq \ell \leq L_i$ in the following graph.

Moreover, for $2 \leq \ell \leq L_i$, any cycle C_t with index $t \in T_{i;\ell}$ has a potential to provide additional $\gamma_{i;t}$ in the ℓ-th level cross parities to v_i. Therefore, $d_{i,\ell} = r_i + \sum_{v_j \in \mathcal{M}_i} \delta_j + \sum_{2\leq \ell' \leq \ell, t \in T_{i,\ell'}} \gamma_{i;t}$. The term $\gamma_{i;t}$ is added to the EC capability if any one of the two nodes v_j and $v_{j'}$, $Y_{t;i} = \{j, j'\}$, obtains its $\gamma_{i;t}$ cross parities at v_i through its $\ell_{t;j}$-th or $\ell_{t;j'}$-th level cooperation. Namely, any one of $\mathbf{m}_i\mathbf{B}_{i,j}$ and $\mathbf{m}_i\mathbf{B}_{i,j'}$ provides the value of $\mathbf{m}_i\mathbf{E}_{i;\ell_{t;i},t}$, and thus provides extra $\gamma_{i;t}$ parity symbols to v_i. Provided that $\mathbf{s}_{j;\ell_{t;j}}$ can be computed if v_j is locally-recoverable, one needs to know the cross parities from all the nodes in the set $\mathcal{I}_j^{\ell_{t;j}} \setminus \{v_i\}$ to obtain those extra $\gamma_{i;t}$ parity symbols, i.e., those nodes are locally-recoverable, which means $\mathcal{I}_j^{\ell_{t;j}} \setminus \mathcal{A}_i^{\ell} \subseteq \{v_i\} \cup \mathcal{W}$. Similarly, the condition of $v_{j'}$ successfully calculating these $\gamma_{i;t}$ cross parities at v_i is described as $\mathcal{I}_{j'}^{\ell_{t;j'}} \setminus \mathcal{A}_i^{\ell} \subseteq \{v_i\} \cup \mathcal{W}$. Therefore, the overall requirement is stated as "$\mathcal{I}_j^{\ell_{t;j}} \setminus \mathcal{A}_i^{\ell} \subseteq \{v_i\} \cup \mathcal{W}$ or $\mathcal{I}_{j'}^{\ell_{t;j'}} \setminus \mathcal{A}_i^{\ell} \subseteq \{v_i\} \cup \mathcal{W}$". From this discussion, we reach that $\mathcal{B}_i^{\ell} = \bigcup_{t\in T_{i;\ell}, j\in Y_{t;i}} (\mathcal{I}_j^{\ell_{t;j}} \setminus (\{v_i\} \cup \mathcal{A}_i^{\ell}))$ and $\lambda_{i,\ell;\mathcal{W}} = r_i + \sum_{j:v_j\in\mathcal{M}_i, (\mathcal{M}_j\setminus\{v_i\})\subseteq(\mathcal{M}_i\cup\mathcal{W})} \delta_j + \sum_{\substack{(i,t):2\leq\ell'\leq\ell, t\in T_{i;\ell'}, Y_{t;i}=\{j,j'\}, \\ \mathcal{I}_j^{\ell_{t;j}}\setminus\mathcal{A}_i^{\ell'}\subseteq(\{v_i\}\cup\mathcal{W}) \text{ or } \mathcal{I}_{j'}^{\ell_{t;j'}}\setminus\mathcal{A}_i^{\ell'}\subseteq(\{v_i\}\cup\mathcal{W})}} \gamma_{i;t}$, for $\varnothing \subseteq \mathcal{W} \subseteq \mathcal{B}_i^{\ell}$. ■

Note that although in a DSN represented by $G(V,E)$, node $v_i \in V$ cooperates with all nodes in $\mathcal{I}_i^{\ell}$ in the ℓ-th level cooperation, $2 \leq \ell \leq L_i$, it is not necessary that all codewords stored in nodes from $\mathcal{I}_i^{\ell}$ need to be recovered. The reason is that these nodes are partitioned into node pairs where the two nodes in the same pair provide exactly the same group of parity symbols and only one of them needs to be recovered for node v_i to recover its codeword, as we discussed in Theorem 3.

For example, suppose Fig. 11 corresponds to a subgraph of a DSN with a recoverable erasure pattern. The pink triangles and the dashed arrows represent the ℓ-th level cooperation at each node such that no other nodes are involved in the ℓ-th level cooperation of these nodes, i.e., C_t is the only cycle in the cycle group containing it. As discussed in Theorem 3, to remove the local cross parities of each node, neighbors of any non-locally-recoverable node should all be locally-recoverable. Therefore, there exists at most one non-locally-recoverable node in each one of the two triangles. For any $i \in X_t$, previous conditions indicate that at least one of the two nodes with indices in $Y_{t;i}$ is locally-recoverable; let it be node v_j, where $j \in Y_{t;i}$. We know that $Y_{t;j}$ consists of i and i' for some $i' \in X_t$ and $i' \neq i$. Since the codeword stored at v_j is locally-recoverable and C_t forms an isolated cycle group, the cross parity $\mathbf{m}_i\mathbf{B}_{i,j} + \mathbf{m}_{i'}\mathbf{B}_{i',j}$ can be derived at node v_j. Since the codeword at $v_{i'}$ is locally-recoverable, $\mathbf{m}_{i'}\mathbf{B}_{i',j}$ can be further subtracted from the cross parity to obtain $\mathbf{m}_i\mathbf{B}_{i,j}$. This observation indicates that regardless of the way the matching graph is specified and the indices of the nodes that are not recovered, the non-recovered nodes are able to obtain their ℓ-th level cross parities. For example, suppose then v_{i_1} and v_{j_1} in Fig. 11 are not locally-recoverable. Since $V_{i_1;\ell} = \{j_1, j_3\}$ and $\mathcal{I}_i^{\ell} = \{v_{j_1}, v_{j_3}\}$, the aforementioned discussion demonstrates that recovering v_{i_1} does not require v_{j_1} to be recovered.

In Fig. 11, the additional erasure correction capabilities offered to the nodes are identical regardless of the structure of the local matching graph. However, this may not be true in general, if more than one cycle gets involved. In general, different local matching graphs are likely to result in non-identical erasure correction capabilities. In particular, although the EC hierarchies are defined by $(\lambda_{i,l;\mathcal{W}})_{\varnothing\subset\mathcal{W}\subset\mathcal{B}_i^{\ell}}$ for each individual node at each cooperation level, this can be more elaborately defined since accessing a different subset of nodes in $\mathcal{I}_i^{l}$ may result in different EC capabilities even if $\mathcal{W}$ are the same, and $\lambda_{i,l;\mathcal{W}}$ only specifies the largest one. We show it in details by Example 9.

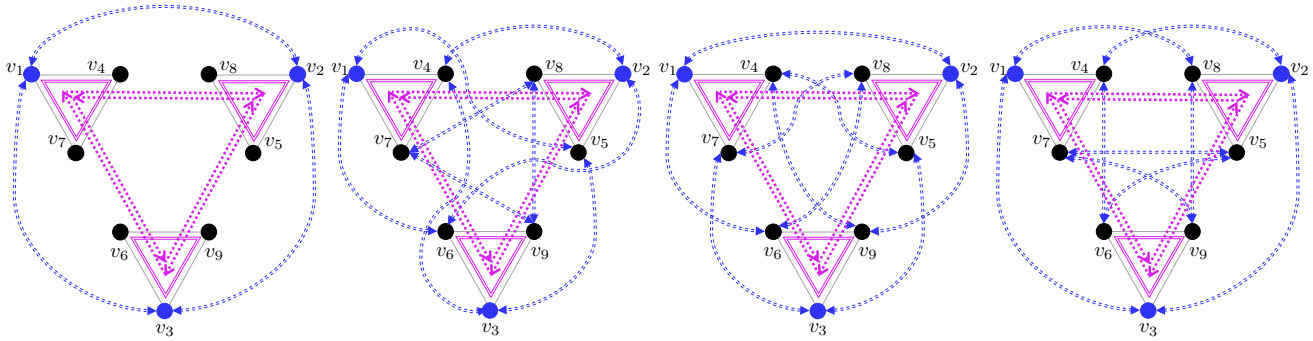


Fig. 14. Possible local matching graphs contained in a multi-level cooperation graph between 9 nodes. The nodes are partitioned into three groups, where nodes within each one of them are pairwisely connected. Each dashed double-sided arrow represent a cycle.

Given an isolated matching graph G', if none of the non-locally-recoverable nodes are able to derive any additional cross parities solely from the local cooperation specified by G', i.e., all cycles in G' constitute a cycle group, we call it an **absorbing matching graph**.

In Example 9, EC capabilities of compatible graphs resulting from the same cooperation graph associated with different local matching graphs, as shown in Fig. 14, are discussed. We prove that the left two panels are two absorbing matching graphs, while the right two panels are not, which also demonstrates that the EC capability is not uniquely determined by the cooperation graph. Instead, the local matching graph also matters.

We focus on the local cooperation graph between 9 nodes in a DSN $G(V, E)$, where $V = \{v_i\}_{i\in[9]}$. Let $V_1 = \{v_1, v_4, v_7\}$, $V_2 = \{v_2, v_5, v_8\}$, and $V_3 = \{v_3, v_6, v_9\}$, and suppose nodes in each one of these sets mutually cooperate with nodes in each of the remaining two sets. According to the definition of cooperation graphs, each one of the graphs represents 3 cycles, $\{C_i\}_{i\in[3]}$, where $X_i = \{3j + i\}_{0\leq j\leq 2}$, $Y_i = X_{i+1}$, and $X_4 = X_1$. Suppose $\{C_i\}_{i\in[3]}$ form an isolated cycle group in the cooperation graph on G. Represent each one of the cycles by a specified matching graph and refer to the resulting local matching graph as an isolated local matching graph. Fig. 14 presents four different isolated local matching graphs on these nodes. Let colors blue and black refer to nodes that are non-locally-recoverable and locally-recoverable nodes, respectively. Then, each V_i, $i \in [3]$, contains at most one blue node if it is contained in a recoverable erasure pattern.

Example 9. (Absorbing Matching Graphs) *Consider the left-most local matching graph in Fig. 14, we notice that v_1, v_2, v_3 are mutually connected (and we will show that the connections between the rest of the nodes actually do not matter, thus we omit them in the figure). Without loss of generality, it is sufficient to prove that v_1 is not able to obtain any extra parity symbols from cycle C_1. Since v_1 and v_2 are connected, we know that $Y_{1;1} = \{5, 8\}$. Thus, v_1 needs to either obtain $\mathbf{m}_1\mathbf{B}_{1,5}$ from v_5 or $\mathbf{m}_1\mathbf{B}_{1,8}$ from v_8. Since v_2 and v_3 are connected, both v_5 and v_8 have cross parities at node v_3. Therefore, the parities v_i, $i \in \{5, 8\}$, are of the form $\mathbf{s}_i = \mathbf{m}_1\mathbf{B}_{1,i} + \mathbf{m}_3\mathbf{B}_{3,i} + \mathbf{m}_j\mathbf{B}_{j,i} + \mathbf{m}_{j'}\mathbf{B}_{j',i}$, where $j \in \{4, 7\}$, $j' \in \{6, 9\}$. If codewords stored at node v_j and $v_{j'}$ are all locally-recoverable, their parities can be subtracted from $\mathbf{s}_i$ to obtain the remainder $\mathbf{s}'_i = \mathbf{m}_1\mathbf{B}_{1,i} + \mathbf{m}_3\mathbf{B}_{3,i}$. Observe that in order to obtain $\mathbf{m}_1\mathbf{B}_{1,i}$, $\mathbf{m}_3\mathbf{B}_{3,i}$ needs to be obtained first. That is to say, v_1 can only obtain additional parities unless the message in v_3 is recovered. However, following a similar process, we will need v_2 to be recovered for v_3, and v_1 to be recovered for v_2. This cyclic requirement indicates that v_1, v_2, and v_3 are "absorbed" into a balanced situation where none of them can be recovered first, which cannot be broken unless information from the rest of the graphs is provided.*

Similarly, we can prove that the second-to-the-left panel is also an absorbing matching graph. Since the connections between the three triangles are symmetric, it is still sufficient to prove that v_1 is not able to obtain any extra parity symbols from cycle C_1. Since v_1 and v_5 are connected, we know that $Y_{1;1} = \{2, 8\}$. Given that v_2 is not locally-recoverable, the only path for v_1 to obtain extra parities is to obtain $\mathbf{m}_1\mathbf{B}_{1,8}$ from v_8. Observe that v_8 is connected to v_7 and v_9 in the matching graph, which means that v_8 has cross parities at v_1, v_3, v_4, and v_6. Therefore, v_8 needs v_3, v_4, and v_6 to be all recovered in order to subtract $\mathbf{m}_3\mathbf{B}_{3,8}$, $\mathbf{m}_4\mathbf{B}_{4,8}$ and $\mathbf{m}_6\mathbf{B}_{6,8}$ from $\mathbf{m}_3\mathbf{B}_{3,8}+\mathbf{m}_4\mathbf{B}_{4,8}+\mathbf{m}_6\mathbf{B}_{6,8}$ to obtain $\mathbf{m}_1\mathbf{B}_{1,8}$. This requires v_3 to be recovered. Following a similar argument to that of the left-most panel, this graph is also an absorbing matching graph.

Moving on to the second-from-the-right panel, v_5 has cross parities at v_7, v_6, v_9, and v_1. Therefore, v_1 is able to obtain the cross parities resulting from cooperation cycle C_3 through v_5. Similarly, v_2 is able to obtain the cross parities resulting from cooperation cycle C_2 through v_4. Finally, v_3 is able to obtain its cross parities from C_3 and C_2.

Now we look at the right-most panel, v_4 has cross parities at v_5, v_8, v_9, and v_3. Therefore, v_3 is able to obtain the cross parities resulting from cooperation cycle C_3 through v_4. Similarly, v_3 is also able to obtain the cross parities resulting from cooperation cycle C_2 through v_5. After that, one of v_1 and v_2 is able to obtain additional parities from C_1, and the other one can obtain additional parities from both C_1 and its cooperation with v_6 and v_9.

Note that the major difference between the second-to-the-right and the right-most panel is that the decoding of v_1 provides no additional parities on v_2 and v_3 in the third one. Therefore, if each cycle C_i, $i \in [3]$, provides η cross parities at each of its nodes, the third and the fourth graphs allow up to additional 4η and 5η cross parities, respectively.

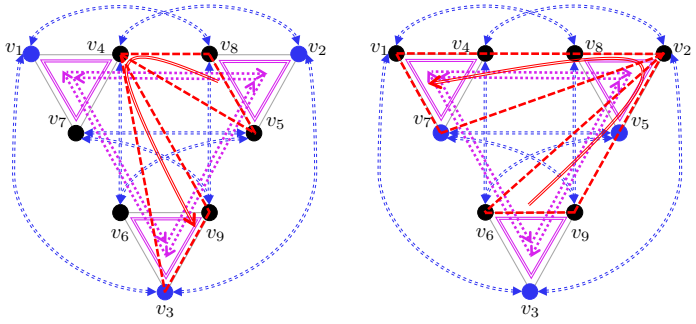


Fig. 15. Information coupling. The two graphs represent two different erasure patterns for the non-absorbing local matching graphs in Fig. 11. While the information flow depicts the communication between any two nodes separated by a distance of 1 or 2 in their 1-st level cooperation, it is not able to fully describe higher level cooperations. Two cycles in a local matching graph also help the decoding of nodes on each other through their shared nodes, and we call this "information coupling".

We have shown in the previous example that the left-most two panels in Figure 11 are absorbing matching graphs, and they become non-absorbing matching graphs if any of the blue nodes turns to be recovered from cooperation with the rest of the graph. In this case, without loss of generality, suppose v_3 is recovered, then v_1 in these two graphs is also recoverable according to discussion in Example 9. While in the left-most panel, nodes in $\mathcal{I}_1^l$ are indeed all locally recovered, those in the second graph from the left are not. We also notice that in the right-most panel, nodes in $\mathcal{I}_1^l$ are locally recovered to recover v_1, while those in the second-to-the right panel are not. Given that any isolated matching graph corresponding to a $\lambda_{1,l;\mathcal{W}}$ with $\mathcal{W} = \varnothing$, this example also demonstrates that a different set $\mathcal{A}_i^l$ will also provide different EC capabilities. While in Example 9 we already subtly discussed such a scenario, we leave more detailed analysis for future work.

Moreover, we state without proof here that the left-most two panels of Fig. 14 discussed in Example 9 are all the possible structures of an absorbing matching graph for this specified local cooperation graph (subject to the graph isomorphism). Since these graphs also are all the possible structures where the nine matching edges form disconnected cycles, those edges in other matching graphs all form a cycle of length 9 and are mutually isomorphic according to permutations of v_1 to v_9. However, different permutations of the nodes do result in different erasure correction capabilities. For example, the second-to-the-right panel is isomorphic to the right-most panel if v_3, v_5, v_7 are blue instead, as shown in Figure 15. This has no impact on the average erasure correction capability while looking into the local matching graphs individually, but the permutation matters while taking the connection to the rest of the graphs into consideration.

In Remark 1, we discuss the information flow between neighboring nodes, and the information flow between nodes with distance two through their common neighbors. Observe that nodes cooperating with any given node in its higher-level cooperations are not necessarily all within its two-hop neighborhood. However, these nodes actually provide additional parities to the original nodes. This scenario is not covered by the previous definition of information flow, instead of it, we proposed the notion of **information coupling** to describe it, as discussed in Remark 2.

Remark 2. (Information Coupling in Multi-Level Coded DSN) *Take the local matching graph shown in the right-most panel in Fig. 11 as an example. Consider the case where non-locally-recoverable nodes are v_1, v_2 and v_3, as shown in the left panel in Fig. 15. Node v_3 is able to obtain additional parities from v_4 since v_5, v_8 and v_9 are locally-recoverable. This case can be regarded as information flow from the cooperation between v_4, v_5 and v_8 to the cooperation between v_4, v_3 and v_9 through v_4.*

Consider another case where the non-locally-recoverable nodes are v_3, v_5 and v_7 instead, as shown in the right panel in Fig. 15. Node v_3 is no longer able to decode its codeword first. Instead, node v_7 is able to obtain additional parities from v_2 since v_1, v_6 and v_9 are locally-recoverable. This case can be regarded as information flow from the cooperation between v_1, v_2, and v_7 to the cooperation between v_2, v_6, and v_9 through v_2.

The aforementioned cases indicate that for any node, nodes cooperating with it in its higher-level cooperation do not have impact on it individually, but rather collectively. Moreover, as discussed in Example 9, this impact is not only dependent on the local matching graphs, but also dependent on the erasure patterns. Therefore, instead of discussing information flow between two cycles, it is more appropriate to treat all the cycles contained in any cycle group collaboratively. This can be interpreted as information coupling resulted from the cooperation between $\{v_1, v_4, v_7\}$, $\{v_2, v_5, v_8\}$, and $\{v_3, v_6, v_9\}$, as an analogy to information coupling in network navigation.

C. Recoverable Erasure Patterns

Recall the notion of "decoding graph" in Definition 2, under which recoverable erasure patterns of the single-level cooperative codes are described. However, in cases where higher-level cooperations are involved, Definition 2 is not enough to define and enumerate all associated recoverable erasure patterns. In this section, we extend Definition 2 into Definition 6 to allow for the multi-level cooperation. Recoverable erasure patterns of hierarchical codes are specified in Theorem 4.

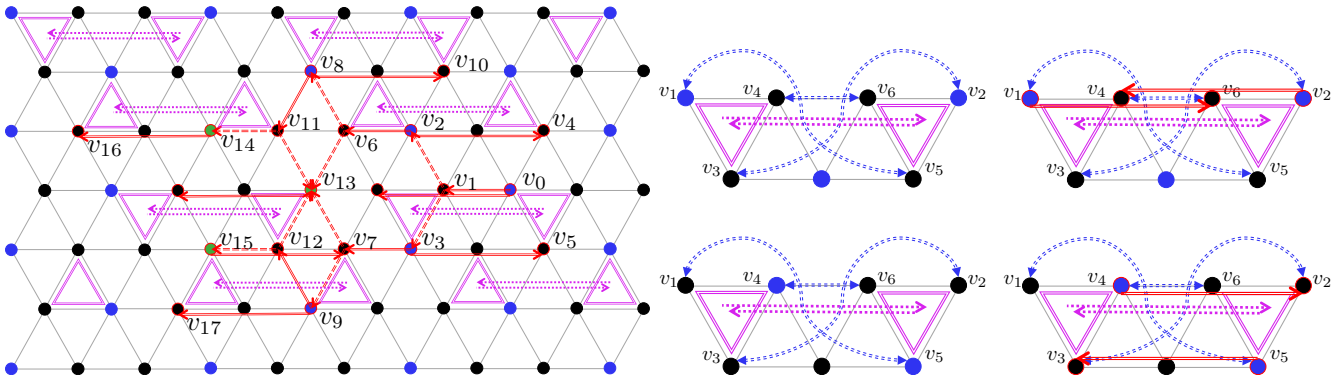


Fig. 16. DSN (left-most) and the local matching graph specified for 2-nd level cooperation in Example 10.

Definition 6. (Decoding Graph in Multi-Level Cooperation) *Let $G(V,E)$ represent a DSN with $|V|=p$. Let $\mathcal{T}(\mathcal{V},\mathcal{E})$ denote a directed subgraph of G associated with $v_j\in\mathcal{V}$. For all $v_i\in\mathcal{V}$, denote the set containing the children of v_i by $\mathcal{V}_i^{\mathrm{C}}$, and the set containing all parents of v_i by $\mathcal{V}_i^{\mathrm{P}}$. Suppose v_j is the only node without parents, we call it the **root** of $\mathcal{T}$. We call any node without children a **leaf**. Suppose that all the leaves of $\mathcal{T}$ are not locally-recoverable, and any other $v_i\in\mathcal{V}$ satisfies either one of the following conditions.*

1) *The codeword stored at v_i is locally-recoverable: there exists a set $\mathcal{L}\subseteq\{2,\ldots,L_i\}$, with $|\mathcal{V}_i^{\mathrm{P}}\cap\mathcal{M}_i|\in\{0,1\}$, $|\mathcal{V}_i^{\mathrm{P}}\cap V_{i;\ell}|=1$, and $\mathcal{V}_i^{\mathrm{P}}\cup\mathcal{V}_i^{\mathrm{C}}$, that consists of all nodes with indices in $V_{i;\ell}$ for $\ell\in\mathcal{L}$ (and $\mathcal{M}_i$ if $|\mathcal{V}_i^{\mathrm{P}}\cap\mathcal{M}_i|=1$), where codewords stored at them are not locally-recoverable.*
2) *The codeword stored at v_i is not locally-recoverable: codewords stored at nodes from $\mathcal{V}_i^{\mathrm{P}}\cup\mathcal{V}_i^{\mathrm{C}}$ are locally-recoverable.*

We call $\mathcal{T}$ a decoding graph at its root node v_j over $G(V,E)$.

Theorem 4. (Flexible Erasure Patterns) *Let $\mathcal{C}$ be a code with hierarchical cooperation on a DSN represented by $G(V,E)$, where $\mathcal{C}$ and all related parameters are specified according to Construction 3. Let $\mathbf{u}\in\mathbb{N}^p$ such that $\mathbf{u}\preceq\mathbf{n}$. Suppose $\mathcal{C}$ and $\mathbf{u}$ satisfy the following conditions:*

1) *Let V^{NL} represent the set contains all the nodes v_i, $i\in[p]$ such that $u_i>r_i-\delta_i$. Let $V^{\mathrm{L}}=V\setminus V^{\mathrm{NL}}$. Then, for any $v_i\in V^{\mathrm{NL}}$, $\mathcal{M}_i\subset V^{\mathrm{L}}$.*
2) *For any $v_i\in V^{\mathrm{NL}}$, there exists a decoding graph $\mathcal{T}_i(\mathcal{V}_i,\mathcal{E}_i)$ at root v_i over G. Moreover, for any leaf v_j of $\mathcal{T}_i$, $u_j\le r_j$; for any node $v_j\in\mathcal{V}_i\cap V^{\mathrm{NL}}$, $u_j\le r_j+\sum_{v_k\in\mathcal{M}_i\cap\mathcal{V}_j^{\mathrm{C}}}\delta_k+\sum_{\ell=2}^{L_i}\sum_{k\in V_{j;\ell}\cap X_{t;j},v_k\in\mathcal{V}_j^{\mathrm{C}}}\gamma_{k;t}$.*

Then, $\mathbf{u}$ is a **recoverable erasure pattern** *of $\mathcal{C}$ over $G(V,E)$.*

Consider the DSN with the 1-st level cooperation graph presented in Example 5. We add the 2-nd level and the 3-rd level cooperation graphs to the DSN and mark them in pink and olive, respectively, as shown in Example 10 and Figure 17. Black and blue/green still refer to nodes where the stored codewords are locally-recoverable and non-locally-recoverable, respectively. Components marked in red represent local decoding graphs, which is the subgraph of the decoding graph corresponding to the local matching graph.

Example 10. *Fig. 16 has five graphs. The left-most panel describes the cooperation graph resulting from adding the 2-nd level cooperation among nodes to the DSN in Example 5, where there exist two possible local matching graphs that are specified by the two graphs in the center (in the central panel). The right-most two panels present the subgraphs in local decoding graphs corresponding to the two possible local matching graphs. Let $\mathbf{u}=(u_1,u_2,\ldots,u_p)$ be an erasure pattern on this DSN. Under the EC solution specified in Theorem 3, suppose there exists $\gamma\in\mathbb{N}$ such that $\gamma_{i;t}=\gamma$, for all $t\in[T]$, and $i\in X_t$.*

In the specified cooperation graph, for $i\in[p]$, if v_i is black, then $0\le u_i\le r_i-\delta-\gamma$; else if v_i is green, then $r_i-\delta-\gamma\le u_i\le r_i+\gamma$; otherwise $r_i+\gamma<u_{1,i}\le r_i+\delta+\gamma$. Since each blue node is contained in an isolated local matching graph, it can obtain additional γ cross parity symbols from its 2-nd level cooperation according to the previous discussion about Fig. 11. Therefore, all the non-locally-recoverable nodes are able to tolerate extra γ erasures, which means that $\mathbf{u}$ is a recoverable erasure pattern of this graph but not a recoverable pattern of the left panel in Fig. 6.

Example 11. *Fig. 17 has three graphs. The left-most one describes the cooperation graph resulting from adding the 2-nd and the 3-rd level cooperations among nodes to the DSN in Example 5. We adopt the right-most local matching graph in Fig. 14 to specify local matching graphs in this example, and it is shown in the central panel. Note that we have exchanged the indices of v_4 and v_7, and those of v_5 and v_8 in the original graph to obtain the graph in the center. The right-most panel presents the subgraph in local decoding graphs corresponding to the local matching graph. Let $\mathbf{u}=(u_1,u_2,\ldots,u_p)$ be an erasure pattern on this DSN. Under the EC solution specified in Theorem 3, suppose there exists $\gamma\in\mathbb{N}$ such that $\gamma_{i;t}=\gamma$, for all $t\in[T]$, and $i\in X_t$.*

In the specified cooperation graph, for $i\in[p]$, if v_i is black and is connected to two triangles, then $0\le u_i\le r_i-\delta-2\gamma$; else if v_i is black and is connected to only one triangle, then $0\le u_i\le r_i-\delta-\gamma$; else if v_i is blue and is connected to only one

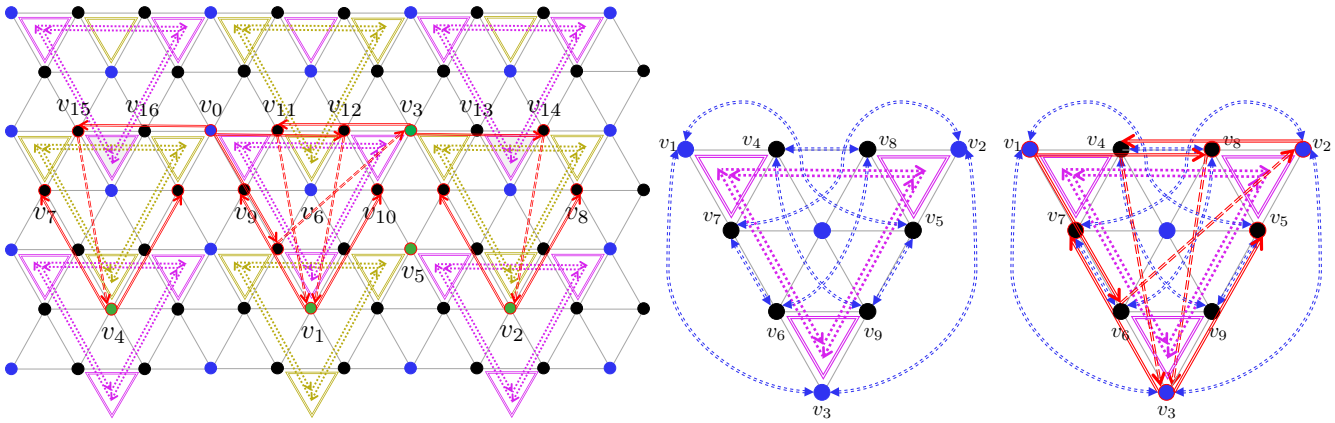


Fig. 17. DSN (left-most) and the local matching graph specified for 2-nd and 3-rd level cooperation in Example 11.

triangle, $r_i-\delta-\gamma < u_{1,i} \leq r_i+2\gamma$; else if v_i is green, then $r_i-\delta-2\gamma < u_i \leq r_i+2\gamma$; otherwise $r_i-\delta-2\gamma < u_{1,i} \leq r_i+3\gamma$. Since each non-locally-recoverable node, e.g., v_1, v_2, and v_4, is contained in an isolated local matching graph, i.e., a triangle, laying at the bottom of this triangle, it can obtain additional 2γ cross parity symbols from it according to the previous discussion in Example 9. Then, v_3 and v_5 can also obtain extra 2γ parity symbols, where γ of them are from the 2-nd level cooperation, and the remaining γ of them are from the 3-rd level cooperation, respectively, according to Example 9. After that v_0 is able to obtain 2γ cross parity symbols from the 2-nd level cooperation (the pink triangle), and γ cross parity symbols from the 3-rd level cooperation (the olive triangle). Following a similar logic, all codewords in the non-locally-recoverable nodes are able to be recovered, which means that $\mathbf{u}$ is a recoverable erasure pattern of this graph but not a recoverable pattern of any of the graphs in Fig. 6.

V. Topology Adaptivity, Scalability, and Flexibility

In Section IV, we have presented a construction of codes with hierarchical locality for a DSN with a given cooperation graph, which enables the system to offer multi-level access at each node while simultaneously reducing the latency by taking into account the communication cost between different nodes. However, multi-level accessibility is not the only property that is desirable in practical cloud storage applications. In this section, we therefore discuss topology adaptivity, scalability, and flexibility of our construction, which are especially critical in dynamic cloud storage.

A. Topology Adaptivity

As discussed in Section I, varying topology is a critical property of DSNs because of the dynamic nature of practical networks. While discussing EC solutions for DSNs with a specific topology, the time cost in each communication link and the erasure statistics of each node should also be taken into consideration to have a good trade-off between low latency and high EC capability. Although hierarchical coding schemes over a DSN with a specified cooperation graph has been discussed in Subsection IV-A, the method of finding a cooperation graph over DSNs with arbitrary topology has not yet been discussed. Algorithm 1 searches for a cooperation graph over a given network; the existence of such a graph is implicitly proved in the algorithm. Here $G(V, E)$ denotes a DSN with the collection $S(V, E)$ of maximum cliques.

Remark 3. *(Latency Optimization in Cooperation Graphs) One might observe that although Algorithm 1 presents a general method to search for a cooperation graph over a given DSN described by $G(V, E)$, the resulting code is not guaranteed to possess optimized latency. Optimization of the construction with the lowest latency is left for future work.*

B. Scalability

As discussed in Section I, scalability refers to the capability of expanding the backbone network to accommodate additional workload without rebuilding the entire infrastructure. More specifically, when a new cloud is added to the existing configuration, computing a completely different generator matrix results in changing all the encoding-decoding components in the system, and is very costly. The preferred scenario is that adding a new cloud does not change the encoding-decoding components of the existing clouds.

Algorithm 1 Cooperation Graph Search

Inputs:

$G(V, E)$: existing DSN;

$a(S)$: the number of different cycle groups associated with the maximum clique $S \in S(V, E)$;

$b(g)$: the number of cycles within the cycle group g;

Outputs:

$\mathcal{G}(\mathcal{V}, \mathcal{E})$: a cooperation graph over G;

//Find a cooperation graph

$\mathcal{V} \leftarrow V$, $\mathcal{E} \leftarrow \varnothing$;
for $v_i \in V$ **do**
  Assign a subset of $\mathcal{N}_i$ to $\mathcal{M}_i$;
  $\mathcal{E} \leftarrow \mathcal{E} \cup \{e_{i,j} : v_j \in \mathcal{M}_i\}$;
end for
Find the collection $\mathcal{S}(\mathcal{V}, \mathcal{E})$ of maximum cliques over $\mathcal{G}$;
$t \leftarrow 1$, $g \leftarrow 1$;
for $S \in \mathcal{S}(\mathcal{V}, \mathcal{E})$ **do**
  for $1 \le i \le a(S)$ **do**
    for $1 \le b \le b(g)$ **do**
      Find an edge or a triangle contained in S and denote the set consisting of indices of its vertices by Y_t;
      Find another edge in G if $|Y_t| = 2$; else find a triangle such that there exists a bijection f from X_t to Y_t and $\{e_{i,j}\}_{(i,j)\in X_t \times Y_t \setminus \{(i,f(i)):i\in X_t\}} \subseteq \bar{\mathcal{E}}$, where X_t denotes the set consisting of indices of its vertices;
      $\mathcal{E} \leftarrow \mathcal{E} \cup \{e_{i,j}\}_{(i,j)\in X_t \times Y_t \setminus \{(i,f(i)):i\in X_t\}}$;
      $X_{t;j} \leftarrow X_t \setminus \{f^{-1}(j)\}$, $Y_{t;i} \leftarrow Y_t \setminus \{f(i)\}$, $g_t \leftarrow g$, $l_{t;i} \leftarrow 0$, for $i \in X_t$, $j \in Y_t$;
      Add $C_t(X_t, Y_t, \{X_{t;j}\}_{j\in Y_t}, \{Y_{t;i}\}_{i\in X_t}, g_t, (l_{t;j})_{j\in Y_t})$ to $\mathcal{G}$;
      $t \leftarrow t + 1$;
    end for
    $g \leftarrow g + 1$;
  end for
end for

//Assign associated cooperation levels to $\mathcal{G}$, following the notation specified in Table II

for $v_i \in V$ **do**
  Find the set A_i consisting of group numbers of those cycle groups that contain at least a cycle C_t with $i \in Y_t$;
  for $g \in A_i$ **do**
    Find the set $R_{i;g}$ consisting of all cycles C_t such that $g_t = g$ and $i \in Y_t$;
    Denote the average distance of all nodes v_j, $j \in X_{t;i}$, $t \in R_{i;g}$, by z_i;
  end for
  Order $(z_i)_{i\in[a(S)]}$ from the smallest to the largest, and obtain $(z_{\pi'(i)})_{i\in[a(S)]}$, where $\pi'(i)$ is a permutation of elements from $[a(S)]$;
  for $g \in A_i$ and $t \in R_{i;g}$ **do**
    $l_{t;j} \leftarrow \pi'(i) + 1$, for $j \in X_{t;i}$;
  end for
end for

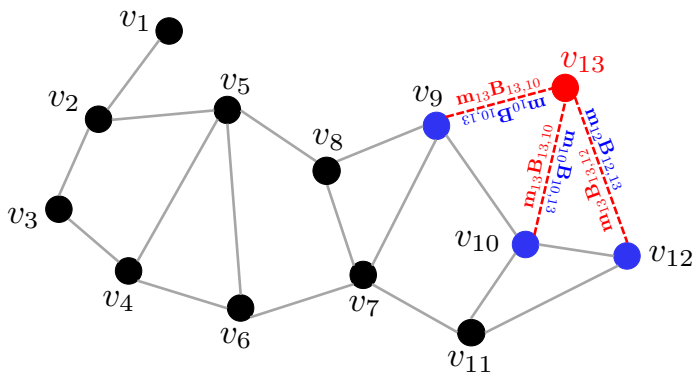


Fig. 18. Scalability: Add a node to existing DSN.

We show that our construction naturally achieves this goal. For simplicity, we only discuss the scalability over constructions with single-level cooperation here. Observe that in Construction 1, the components $\mathbf{A}_{x,x}$, $\mathbf{U}_x$, and $\mathbf{B}_{x,i}$, $i \in [p] \setminus \{x\}$, are built locally. Suppose cloud $p+1$ is added into a double-level configuration adopting Construction 1. Algorithm 2 presents a procedure for adding this cloud, which only results in adding some columns and rows to the original generator matrix without changing the existing ones. Thus, the existing infrastructure does not need to be changed; each node only needs to add cross parities it receives from the newly added node to its current parities. Moreover, with this algorithm, the erasure correction capabilities $\{d_{1,i}\}_{v_i \in \mathcal{N}_{p+1}}$ of neighboring nodes of v_{p+1} are increased by δ_{p+1}.

Algorithm 2 Node Addition

Inputs:

$G(V, E)$: existing DSN;
p: number of nodes in $G(V, E)$;
v_{p+1}: the newly added node;
r_{p+1}: the message length of v_{p+1};
k_{p+1}: the number of parity symbols of the v_{p+1};
δ_{p+1}: the number of additional parities v_{p+1} provides globally to the DSN;
$\mathcal{N}_{p+1}$: the set of nodes to be connected to v_{p+1};
$\mathbf{G}$: the original generator matrix;

Outputs:

$\mathbf{G}$: the updated generator matrix;

1: Node v_{p+1} chooses its local parameters $\mathbf{A}_{p+1,p+1}$, $\mathbf{U}_{p+1}$, and $\mathbf{B}_{p+1,i}$, $v_i \in \mathcal{N}_{p+1}$;
2: Node v_i chooses additional cross parity matrices $\mathbf{B}_{i,p+1}$, $v_i \in \mathcal{N}_{p+1}$;
3: Node v_{p+1} sends $\mathbf{m}_{p+1}\mathbf{B}_{p+1,i}$ to node v_i, $v_i \in \mathcal{N}_{p+1}$;
4: Node v_i sends $\mathbf{m}_i\mathbf{B}_{i,p+1}$ to v_{p+1}, $v_i \in \mathcal{N}_{p+1}$;
5: Node v_{p+1} computes the stored codeword $\mathbf{c}_{p+1} = \mathbf{m}_{p+1}\mathbf{A}_{p+1,p+1} + \sum_{i \in \mathcal{N}} \mathbf{m}_i\mathbf{B}_{i,p+1}\mathbf{U}_{p+1}$;
6: Node v_i adds $\mathbf{m}_{p+1}\mathbf{B}_{p+1,i}$ to its current parity symbols, $v_i \in \mathcal{N}_{p+1}$;
7: Update $\mathbf{G}$ accordingly;

Example 12. *Consider again the set up in Example 2. Suppose a node v_{13} is to be added to the existing DSN and is to be connected to nodes v_9, v_{10}, and v_{12}, as shown in Fig. 18. The messages near the edges marked in red are sent from v_{13}, while those marked in blue are sent from the neighboring nodes v_9, v_{10}, and v_{12}, to v_{13}. Note that the new node v_{13} has coding parameters chosen independently from the existing nodes according to Theorem 1, which means that it naturally achieves scalability.*

C. Flexibility

The concept of flexibility was proposed and investigated for dynamic cloud storage in [26]. In a dynamic cloud storage system, the rate of which a given piece of data is accessed is likely to change. When the data stored at a cloud become hot, i.e., of higher demand, splitting the cloud into two smaller clouds effectively reduces the latency. However, this action should be done without reducing the erasure correction capability of the rest of the system or changing the remaining components.

Specifically, if the data stored at a cloud $v_i \in V$ become unexpectedly hot, the DSN needs to split v_i into two separate smaller clouds $v_{i^{\mathrm{a}}}$ and $v_{i^{\mathrm{b}}}$ to maintain relatively low latency; Algorithm 3 presents the procedure to do this. For simplicity, we focus here on the case where only the 1-st level cooperation is involved in, as presented in Construction 2.

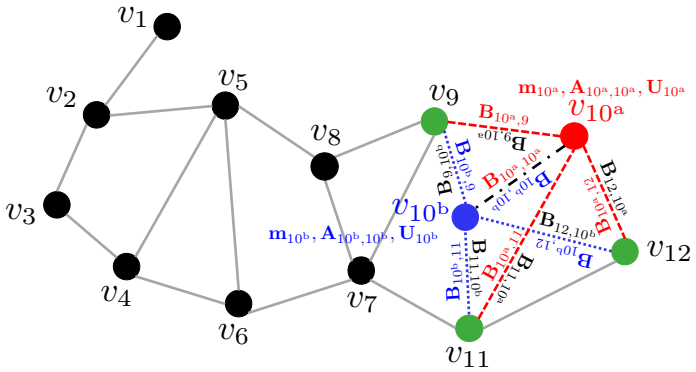


Fig. 19. Flexibility: Split a node to two nodes in a DSN when it gets hot such that accessing the codeword stored at each one of them achieves low latency.

Algorithm 3 Node Splitting

Inputs:

$G(V, E)$: existing DSN;
v_i: the node to be split in $G(V, E)$;
$\mathcal{N}_i$: the set of neighboring nodes of v_i;
$v_{i^{\mathrm{a}}}$, $v_{i^{\mathrm{b}}}$: nodes v_i is split into;
k_i, $k_{i^{\mathrm{a}}}$, $k_{i^{\mathrm{b}}}$: the message lengths of v_i, $v_{i^{\mathrm{a}}}$, $v_{i^{\mathrm{b}}}$, respectively; $k_i = k_{i^{\mathrm{a}}} + k_{i^{\mathrm{b}}}$;
r_i, $r_{i^{\mathrm{a}}}$, $r_{i^{\mathrm{b}}}$: the number of parity symbols of v_i, $v_{i^{\mathrm{a}}}$, $v_{i^{\mathrm{b}}}$, respectively; $r_i = r_{i^{\mathrm{a}}} + r_{i^{\mathrm{b}}}$;
δ_i, $\delta_{i^{\mathrm{a}}}$, $\delta_{i^{\mathrm{b}}}$: the number of additional parities v_i, $v_{i^{\mathrm{a}}}$, $v_{i^{\mathrm{b}}}$ provides globally to the DSN, respectively; $\delta_i = \delta_{i^{\mathrm{a}}} + \delta_{i^{\mathrm{b}}}$;
$\mathbf{G}$: the original generator matrix;

Outputs:

$\mathbf{G}$: the updated generator matrix;

1: Node v_i splits $\mathbf{A}_{i,i}$ into $\mathbf{A}_{i^{\mathrm{a}},i^{\mathrm{a}}}$, $\mathbf{B}_{i^{\mathrm{b}},i^{\mathrm{a}}}$, $\mathbf{A}_{i^{\mathrm{b}},i^{\mathrm{b}}}$, $\mathbf{B}_{i^{\mathrm{a}},i^{\mathrm{b}}}$ as follows:
$\mathbf{A}_{i^{\mathrm{a}},i^{\mathrm{a}}} = \mathbf{A}_{i,i}\left[1 : k_{i^{\mathrm{a}}}, 1 : r_{i^{\mathrm{a}}}\right]$,
$\mathbf{B}_{i^{\mathrm{b}},i^{\mathrm{a}}} = \mathbf{A}_{i,i}\left[k_{i^{\mathrm{a}}} + 1 : k_i, 1 : \delta_{i^{\mathrm{a}}}\right]$,
$\mathbf{A}_{i^{\mathrm{b}},i^{\mathrm{b}}} = \mathbf{A}_{i,i}\left[k_{i^{\mathrm{a}}} + 1 : k_i, r_{i^{\mathrm{a}}} + 1 : r_i\right]$,
$\mathbf{B}_{i^{\mathrm{a}},i^{\mathrm{b}}} = \mathbf{A}_{i,i}\left[1 : k_{i^{\mathrm{a}}}, r_{i^{\mathrm{a}}} + 1 : r_{i^{\mathrm{a}}} + \delta_{i^{\mathrm{b}}}\right]$;
2: Node v_i splits $\mathbf{B}_{i,j}$, $\forall v_j \in \mathcal{N}_i$, into $\mathbf{B}_{i^{\mathrm{a}},j}$ and $\mathbf{B}_{i^{\mathrm{b}},j}$ as follows:
$\mathbf{B}_{i^{\mathrm{a}},j} = \mathbf{B}_{i,j}\left[1 : k_{i^{\mathrm{a}}}, 1 : \delta_j\right]$,
$\mathbf{B}_{i^{\mathrm{b}},j} = \mathbf{B}_{i,j}\left[k_{i^{\mathrm{a}}} + 1 : k_i, 1 : \delta_j\right]$;
3: Node v_j, $\forall v_j \in \mathcal{N}_i$, splits $\mathbf{B}_{j,i}$ into $\mathbf{B}_{j,i^{\mathrm{a}}}$ and $\mathbf{B}_{j,i^{\mathrm{b}}}$ as follows:
$\mathbf{B}_{j,i^{\mathrm{a}}} = \mathbf{B}_{j,i}\left[1 : k_j, 1 : \delta_{i^{\mathrm{a}}}\right]$,
$\mathbf{B}_{j,i^{\mathrm{b}}} = \mathbf{B}_{j,i}\left[1 : k_j, \delta_{i^{\mathrm{a}}} + 1 : \delta_i\right]$, $\forall v_j \in \mathcal{N}_i$;
4: Node v_i splits $\mathbf{U}_i$ into $\mathbf{U}_{i^{\mathrm{a}}}$ and $\mathbf{U}_i^{\mathrm{b}}$ as follows:
$\mathbf{U}_{i^{\mathrm{a}}} = \mathbf{U}_i\left[1 : \delta_{i^{\mathrm{a}}}, 1 : r_{i^{\mathrm{a}}}\right]$,
$\mathbf{U}_{i^{\mathrm{b}}} = \mathbf{U}_i\left[\delta_{i^{\mathrm{a}}} + 1 : \delta_1, r_{i^{\mathrm{a}}} + 1 : r_{i^{\mathrm{b}}}\right]$;
5: Compute the additional cross parities $\mathbf{s}_i$'s by solving the equation $\mathbf{s}_i\mathbf{U}_i = \mathbf{c}_i - \mathbf{m}_i\mathbf{A}_{i,i}$, where $i \in [p]$. Find $\mathbf{s}_{i^{\mathrm{a}}} \in \mathrm{GF}(q)^{\delta_{i^{\mathrm{a}}}}$, $\mathbf{s}_{i^{\mathrm{b}}} \in \mathrm{GF}(q)^{\delta_{1^{\mathrm{b}}}}$ such that $\mathbf{s}_i = [\mathbf{s}_{i^{\mathrm{a}}}, \mathbf{s}_{i^{\mathrm{b}}}]$;
6: Compute the message stored at the node $v_{i^{\mathrm{a}}}$ and $v_{i^{\mathrm{a}}}$ as follows:
$\mathbf{c}_{i^{\mathrm{a}}} = \left[\mathbf{m}_{i^{\mathrm{a}}}, \mathbf{m}_{i^{\mathrm{a}}}\mathbf{A}_{i^{\mathrm{a}},i^{\mathrm{a}}} + \left(\mathbf{m}_{i^{\mathrm{b}}}\mathbf{B}_{i^{\mathrm{b}},i^{\mathrm{a}}} + \mathbf{y}_{i^{\mathrm{a}}}\right)\mathbf{U}_{i^{\mathrm{a}}}\right]$,
$\mathbf{c}_{i^{\mathrm{b}}} = \left[\mathbf{m}_{i^{\mathrm{b}}}, \mathbf{m}_{i^{\mathrm{b}}}\mathbf{A}_{i^{\mathrm{b}},i^{\mathrm{b}}} + \left(\mathbf{m}_{i^{\mathrm{a}}}\mathbf{B}_{i^{\mathrm{a}},i^{\mathrm{b}}} + \mathbf{y}_{i^{\mathrm{b}}}\right)\mathbf{U}_{i^{\mathrm{b}}}\right]$;
7: Update $\mathbf{G}$ accordingly;

Note that the matrix $\mathbf{B}_{i,j}$ is vertically split into $\mathbf{B}_{i^{\mathrm{a}},j}$ and $\mathbf{B}_{i^{\mathrm{b}},j}$, while $\mathbf{B}_{j,i}$ is horizontally split into $\mathbf{B}_{j,i^{\mathrm{a}}}$ and $\mathbf{B}_{j,i^{\mathrm{b}}}$, for all v_j that are neighboring nodes of v_i. Therefore, it is obvious that $\mathbf{m}_i\mathbf{B}_{i,j} = \mathbf{m}_{i^{\mathrm{a}}}\mathbf{B}_{i^{\mathrm{a}},j} + \mathbf{m}_{i^{\mathrm{b}}}\mathbf{B}_{i^{\mathrm{b}},j}$ and one can prove that the local codeword $\mathbf{c}_j$ doesn't change for v_j that is a neighboring node of v_i. Moreover, since both the local and the global parity-check matrices for each non-split cloud remain unchanged, the local and global erasure capabilities of them are not affected according to Lemma 2. Furthermore, one can prove that the local codewords stored at the new clouds i^{a} and i^{b} tolerate $(r_{i^{\mathrm{a}}} - \delta_{i^{\mathrm{a}}})$ and $(r_{i^{\mathrm{b}}} - \delta_{i^{\mathrm{b}}})$ local erasures, respectively.

Example 13. *Consider again Example 2. If the data stored at node v_{10} become unexpectedly hot, then we split v_{10} into two separate nodes $v_{10^{\mathrm{a}}}$ and $v_{10^{\mathrm{b}}}$ following Algorithm 3, as shown in Fig. 19.*

Originally, node v_{10} needs to access all $n_{10} = k_{10} + r_{10}$ symbols to obtain message $\mathbf{m}_{10}$, which results in high latency when one has to access any set of symbols from $\mathbf{m}_{10}$ frequently. This operation results in unnecessary cost in terms of data processing times, which can be solved by splitting v_{10} into two nodes $v_{10^{\mathrm{a}}}$ and $v_{10^{\mathrm{b}}}$ that store $n_{10^{\mathrm{a}}} = k_{10^{\mathrm{a}}} + r_{10^{\mathrm{a}}}$ and $n_{10^{\mathrm{b}}} = k_{10^{\mathrm{b}}} + r_{10^{\mathrm{b}}}$ symbols, which contain the information of $\mathbf{m}_{10^{\mathrm{a}}}$ and $\mathbf{m}_{10^{\mathrm{b}}}$, respectively. Local access to each one of the two nodes will require significantly lower latency compared with a full access of the original node v_{10}. This approach improves the latency especially if the erasures are bursty, i.e., concentrated within any one of $\mathbf{c}_{10^{\mathrm{a}}}$ or $\mathbf{c}_{10^{\mathrm{b}}}$. Even if the erasures are distributed more evenly among $\mathbf{c}_{10^{\mathrm{a}}}$ and $\mathbf{c}_{10^{\mathrm{b}}}$, the total processing time to obtain $\mathbf{m}_{10}$ will be the maximum of their individual processing times, which is still much shorter than the original time.

VI. Conclusion

Hierarchical locally accessible codes in the context of centralized cloud networks have been discussed in various prior works, whereas those of DSNs (no prespecified topology) have not been explored. In this paper, we proposed a topology-adaptive cooperative data protection scheme for DSNs, which significantly extends our previous work on hierarchical coding for centralized distributed storage. We discussed the recoverable erasure patterns of our proposed scheme, demonstrating that our scheme corrects patterns pertaining to dynamic DSNs. Our scheme achieves faster recovery speed compared with existing network coding methods, and enables an intrinsic information flow from nodes with higher reliability to nodes with lower

reliability that are close to them on the network. Moreover, our constructions are also proved to be scalable and flexible, making them a construction with great potential to be employed in dynamic DSNs.

ACKNOWLEDGMENT

This work was supported in part by NSF under the grants CCF-BSF 1718389 and CCF 1717602, and in part by AFOSR under the grant FA 9550-17-1-0291.

REFERENCES

[1] S. Yang, A. Hareedy, R. Calderbank, and L. Dolecek, "Hierarchical coding to enable scalability and flexibility in heterogeneous cloud storage," in *IEEE Global Communications Conference (GLOBECOM)*, Dec. 2019. [Online]. Available: https://arxiv.org/abs/1905.02279

[2] ——, "Topology-aware cooperative data protection in blockchain-based decentralized storage networks," 2020. [Online]. Available: https://arxiv.org/abs/2001.04526

[3] "Storj: A decentralized cloud storage network framework," Oct. 2018. [Online]. Available: https://storj.io/storjv3.pdf

[4] M. Hassner, K. Abdel-Ghaffar, A. Patel, R. Koetter, and B. Trager, "Integrated interleaving-a novel ECC architecture," *IEEE Transactions on Magnetics*, vol. 37, no. 2, pp. 773–775, Feb. 2001.

[5] P. Huang, E. Yaakobi, and P. H. Siegel, "Multi-erasure locally recoverable codes over small fields," in *55th Annual Allerton Conference on Communication, Control, and Computing (Allerton)*. IEEE, Sep. 2017, pp. 1123–1130.

[6] Y. Cassuto, E. Hemo, S. Puchinger, and M. Bossert, "Multi-block interleaved codes for local and global read access," in *Proceedings IEEE Int. Symp. Inf. Theory*, 2017, pp. 1758–1762.

[7] Y. Wu, "Generalized integrated interleaved codes," *IEEE Transactions on Information Theory*, vol. 63, no. 2, pp. 1102–1119, Nov. 2017.

[8] S. Ballentine, A. Barg, and S. Vladuts, "Codes with hierarchical locality from covering maps of curves," 2018. [Online]. Available: https://arxiv.org/abs/1807.05473

[9] X. Zhang, "Generalized three-layer integrated interleaved codes," *IEEE Communications Letters*, vol. 22, no. 3, pp. 442–445, Mar. 2018.

[10] M. Blaum and S. R. Hetzler, "Extended product and integrated interleaved codes," *IEEE Transactions on Information Theory*, vol. 64, no. 3, pp. 1497–1513, Mar. 2018.

[11] S. B. Balaji, G. R. Kini, and P. V. Kumar, "A tight rate bound and matching construction for locally recoverable codes with sequential recovery from any number of multiple erasures," *IEEE Transactions on Information Theory*, vol. 66, no. 2, pp. 1023–1052, 2020.

[12] A. G. Dimakis, P. B. Godfrey, Y. Wu, M. J. Wainwright, and K. Ramchandran, "Network coding for distributed storage systems," *IEEE Transactions on Information Theory*, vol. 56, no. 9, pp. 4539–4551, Sep. 2010.

[13] Z. Kong, S. A. Aly, and E. Soljanin, "Decentralized coding algorithms for distributed storage in wireless sensor networks," *IEEE Journal on Selected Areas in Communications*, vol. 28, no. 2, pp. 261–267, Feb. 2010.

[14] M. Ye and A. Barg, "Cooperative repair: Constructions of optimal MDS codes for all admissible parameters," *IEEE Transactions on Information Theory*, vol. 65, no. 3, pp. 1639–1656, Mar. 2018.

[15] A. Tebbi, T. H. Chan, and C. W. Sung, "Multi-rack distributed data storage networks," *IEEE Transactions on Information Theory*, vol. 65, no. 10, pp. 6072–6088, Oct. 2019.

[16] H. Hou, P. P. C. Lee, K. W. Shum, and Y. Hu, "Rack-aware regenerating codes for data centers," *IEEE Transactions on Information Theory*, vol. 65, no. 8, pp. 4730–4745, Aug. 2019.

[17] Z. Chen and A. Barg, "Explicit constructions of MSR codes for clustered distributed storage: The rack-aware storage model," 2019. [Online]. Available: https://arxiv.org/abs/1901.04419

[18] N. Prakash, V. Abdrashitov, and M. Médard, "The storage versus repair-bandwidth trade-off for clustered storage systems," *IEEE Transactions on Information Theory*, vol. 64, no. 8, pp. 5783–5805, Aug. 2018.

[19] J. Li, S. Yang, X. Wang, and B. Li, "Tree-structured data regeneration in distributed storage systems with regenerating codes," in *Proceedings of 2010 IEEE INFOCOM*, 2010, pp. 1–9.

[20] J. Pernas, C. Yuen, B. Gastón, and J. Pujol, "Non-homogeneous two-rack model for distributed storage systems," in *IEEE International Symposium on Information Theory*, Jun. 2013, pp. 1237–1241.

[21] Y. Wang, D. Wei, X. Yin, and X. Wang, "Heterogeneity-aware data regeneration in distributed storage systems," in *Proceedings of 2010 IEEE INFOCOM*, 2014, pp. 1878–1886.

[22] A. M. Ibrahim, A. A. Zewail, and A. Yener, "Green distributed storage using energy harvesting nodes," *IEEE Journal on Selected Areas in Communications*, vol. 34, no. 5, pp. 1590–1603, May 2016.

[23] M. Sipos, J. Gahm, N. Venkat, and D. Oran, "Network-aware feasible repairs for erasure-coded storage," *IEEE/ACM Transactions on Networking*, vol. 26, no. 3, pp. 1404–1417, Mar. 2018.

[24] ——, "Erasure coded storage on a changing network: The untold story," in *IEEE Global Communications Conference (GLOBECOM)*, Dec. 2016, pp. 1–6.

[25] B. P. Rimal, E. Choi, and I. Lumb, "A taxonomy and survey of cloud computing systems," in *5th International Joint Conference on INC, IMS and IDC*, Aug. 2009, pp. 44–51.

[26] U. Martnez-Penas and F. R. Kschischang, "Universal and dynamic locally repairable codes with maximal recoverability via sum-rank codes," in *56th Annual Allerton Conference on Communication, Control, and Computing (Allerton)*, Oct. 2018, pp. 792–799.

[27] J. Van Lint and R. Wilson, "On the minimum distance of cyclic codes," *IEEE Transactions on Information Theory*, vol. 32, no. 1, pp. 23–40, Jan. 1986.

[28] J. Bloemer, M. Kalfane, R. Karp, M. Karpinski, M. Luby, and D. Zuckerman, "An XOR-based erasure-resilient coding scheme," 1995.

[29] J. S. Plank and L. Xu, "Optimizing Cauchy Reed-Solomon codes for fault-tolerant network storage applications," in *5th IEEE International Symposium on Network Computing and Applications (NCA'06)*, Jul. 2006, pp. 173–180.

[30] S. Wu, Y. Xu, Y. Li, and Z. Yang, "I/O-efficient scaling schemes for distributed storage systems with CRS codes," *IEEE Transactions on Parallel and Distributed Systems*, vol. 27, no. 9, pp. 2639–2652, Sep. 2015.

[31] Y. Zhu, C. Lv, Z. Zeng, J. Wang, and B. Pei, "Blockchain-based decentralized storage scheme," in *Journal of Physics: Conference Series*, vol. 1237, no. 4, Apr. 2019, p. 042008.

[32] S. Underwood, "Blockchain beyond bitcoin," *Communications of the ACM*, no. 11, Nov. 2016.